Conditional Generative Adversarial Networks With Cascaded U-Net As The Generative Network For Multimodal Brain Tumour Segmentation

Sushma Podishetti
(Student Id: 931050)
M.Sc. in Data Science,
Liverpool John Moore's University
Supervisor: Shah Ayub Quadri

Interim Report

NOVEMBER 2020

ABSTRACT

The most commonly occurring tumours in the brain that originate from glial cells and infiltrate the tissues surrounding them are gliomas. Gliomas are inherently heterogeneous concerning their histology, shape, and appearance. Because of their heterogeneous nature, it is very challenging to segment gliomas sub-regions in Magnetic Resonance Imaging (MRI) scans. Replacing the traditional procedures with the methods that are the state-of-the-art for segmentation of glioma sub-regions in the MRI scans would be of great value for better diagnosis, treatment planning. It would also save doctors time. This paper proposes a state-of-the-art neural network architecture that is based on the Conditional Generative Adversarial Network (CGAN) for the automatic segmentation of glioma sub-regions. The CGANs can accurately segment the tumour with its generator and discriminator network. The generative network learns the inherent heterogeneity of gliomas and challenges the adversarial network on its ability to differentiate between real and generated images. The adversarial network challenges the generative network by segmenting the tumours accurately. This results in improved accuracy of the segmentation. Experiments will be performed on multimodal MRI brain scans from the BraTS 2020 challenge. The model is expected to segment glioma sub-regions (the enhancing tumour (ET), the peritumoral edema (ED), the non-enhancing tumour core (NET), and the necrotic (NCR)). The metrics Dice score, specificity, sensitivity, and Hausdorff distance will be used to assess the performance of the model.

Keywords:

Brain Tumour Segmentation, Gliomas, MRI, Conditional Generative Adversarial Network,

U-Net, CGAN, Glioma sub-regions

TABLE OF CONTENTS

ABSTRACT ii

LIST OF TABLES v

LIST OF FIGURES vi

LIST OF EQUATIONS vii

LIST OF ABBREVIATIONS viii

CHAPTER 1 1

INTRODUCTION 1

1.1 Background 1

1.1.1 Gliomas 1

1.1.2 Dataset 2

1.2 Problem Statement 2

1.3 Research Questions 2

1.4 Aim and Objectives 2

1.5 Significance of this study 3

1.6 Scope of this study 3

1.7 Structure of the study 3

CHAPTER 2 5

LITERATURE REVIEW 5

2.1 Introduction 5

2.2 Brain Tumours 5

2.2.1 Brain Anatomy and Types of Tumours 5

2.2.2 Risk Factors 6

2.2.3 Symptoms 6

2.2.4 Diagnosis 6

2.2.5 Treatment 6

2.3 Data Format 7

2.4 Evaluation Metrics 8
2.5 Image Segmentation 8
2.6 Brain Tumour Segmentation 10
2.7 Benchmarks & Surveys 15
2.8 Discussion 18
2.9 Summary 19
CHAPTER 3 21
RESEARCH METHODOLOGY 21
3.1 Introduction 21
3.2 Research Process 21
3.3 Research Approach 23
3.3.1 Data Selection 24
3.4 Proposed Model 28
3.4.1 Conditional Adversarial Networks 28
3.4.2 U-Net 30
REFERENCES 34
APPENDIX A: RESEARCH PLAN 41
APPENDIX B: RESEARCH PROPOSAL 42
APPENDIX C: SUMMARY OF BRATS 2012 TO 2019 **Error! Bookmark not defined.**

LIST OF TABLES

Table 2.1: Details of NIfTI file format 8
Table 2.2: Results obtained by the model proposed by Sérgio Pereira et al. on 11
Table 2.3: Results obtained by the model proposed by Sérgio Pereira et al. on 11
Table 2.4: Results obtained by the model proposed by Mina Rezaei et al. on 12
Table 2.5: Results obtained by the model proposed by Hao Dong et al. on 13
Table 2.6: Results obtained by the model proposed by Shaoguo Cui et al. 13
Table 2.7: Results achieved by OM-Net + CGA^{p} proposed by Chenhong Zhou et al. 14
Table 2.8: Results obtained by Dmitry Lachinov et al. on BraTS 2018 dataset ..... **Error! Bookmark not defined.**
Table 2.9: Results obtained by Mohammad Havaeia et al. on BraTS 2013 test data set 15

LIST OF FIGURES

Figure 2.1: The graph of segmentation accuracies achieved by top-performing models.....18
Figure 3.1: Flow chart representing the research process 22
Figure 3.2: Proposed research approach - Model: CGAN with cascaded U-Net as the generator 23
Figure 3.3: Different image modalities of the brain from BraTS dataset(Jiang et al., 2020a) .24
Figure 3.4: Sections of brain images with gliomas sub-regions in different MRI modalities (http://braintumoursegmentation.org/ 25
Figure 3.5: Illustration of a simple CGAN 29
Figure 3.6: Simple representation of Conditional Generative Adversarial Network 30

LIST OF EQUATIONS

Equation 3.1:Dice score formula 26
Equation 3.2: Sensitivity formula 27
Equation 3.3: Specificity formula 27
Equation 3.4: Hausdorff distance formula 27
Equation 3.5: Directed Hausdorff distance formula 27
Equation 3.6: Minmax loss function used by CGANS 29

LIST OF ABBREVIATIONS

Abbreviation	Full form
MRI	Magnetic Resonance Imaging
CGAN	Conditional Generative Adversarial Network
ET	Enhancing Tumour
ED	Edema
NET	Non-Enhancing Tumour Core
NCR	Necrotic
CT	Computed Tomography
HGG	High-Grade Gliomas
LGG	Low-Grade Gliomas
BraTS	Brain Tumour Segmentation
3D	Three Dimensional
IOU	Intersection Over Union
EM	Electron Microscopic
ISBI	International Symposium on Biomedical Imaging
CNN	Convolutional Neural Network
PReLu	Parametric Rectified Linear Unit
ROI	Region of Interest
DDSM	Digital Database for Screening Mammography
LReLu	Leaky Rectified Linear Unit
ReLU	Rectified Linear Unit
GAN	Generative Adversarial Network
RNN	Recurrent Neural Network
TLN	Tumour Localization Network
ITCN	Intratumor Classification Network
FCN	Fully Convolutional Network
DSC	Dice Similarity Coefficient
PPV	Positive Predictive Value
MC	Model Cascade
OM-Net	One-pass Multi-task Network
CGA	Cross-task Guided Attention
SE	Squeeze-and Excitation

Abbreviation	Full form
CF	Classification Forest
ANT	Advanced Normalization Tools
GMM	Gaussian Mixture Modeling
RF	Random Forests
MAP	Maximum a Posteriori Estimate
MRF	Markov Random Fields
2D	Two Dimensional
CSF	Cerebrospinal Fluid
EMMA	Ensemble of Multiple Models and Architectures
ResNet	Residual Network
VAE	Variational Auto-encoder
FCM	Fuzzy C-Means
ANN	Artificial Neural Network
SVM	Support Vector Machines
RECIST	Response Evaluation Criteria in Solid Tumours
RANO	Response Assessment in Neuro-Oncology
ML	Machine Learning
GBM	Glioblastoma Multiforme
GPU	Graphics Processing Unit
Gd	Gadolinium
FLAIR	Fluid Attenuated Inversion Recovery
TC	Tumour Core
WT	Whole Tumour
TPR	True Positive Rate
TNR	True Negative Rate
HD	Hausdorff Distance
DIC	Differential Interference Contrast
NIfTI	Neuroimaging Informatics Technology Initiative

CHAPTER 1

INTRODUCTION

This chapter gives a background on gliomas, the brain tumours on which this research focuses and the dataset used in this research. The reasons for doing this research It states the problem this research would address, the questions the research would answer, the aims and objectives of this research. It presents the significance, scope and structure of this study

1.1 Background

This section focuses on glioma and its sub-regions, the methods of diagnosing gliomas, the different grades of gliomas. It gives the details of the dataset used in this research. As it is time consuming, tedious, and requires a lot of attention to segment the gliomas sub-regions manually, it becomes extremely important to fully automate this process for improved diagnosis, treatment planning, follow-up and to assess the way the tumour progresses. It would also save doctors time (Lachinov et al., 2020). This paper proposes a neural network architecture based on CGAN with U-Net as the generator for improved segmentation of glioma sub-regions.

1.1.1 Gliomas

This study focuses on the segmentation of glioma sub-regions. These brain tumours start from the glial cells. Glial cells support the function of the neurons. They commonly occur in the cerebral hemispheres of the brain. They can be benign or malignant. The exact cause of gliomas is not known. They contribute about one-third of all brain tumours.

Gliomas are diagnosed based on medical history, physical examination, neurological examination, images of the brain, and biopsy. MRI and CT scans are used most commonly to diagnose brain tumours and to check for tumour growth after the treatment.

Gliomas are classified into grades I, II, III & IV. These four grades of gliomas are grouped into "Low-Grade Gliomas (LGG)" (grade I or grade II) and "High-Grade Gliomas (HGG)" (grade III or grade IV) based on the tumour's aggressiveness and growth potential. The treatment for gliomas depends on its grade. The patients with HGG can survive for two years or less and would need treatment immediately. The patients with LGG can survive for several years, and aggressive treatment can be delayed. For both grades of gliomas, multimodal brain

images are used before and after treatment to diagnose, check the tumour progression, and to evaluate the treatment strategy.

1.1.2 Dataset

The experiment will be performed on the brain MRI scans from BraTS 2020 challenge. The data set contains a training set and a validation set. The training dataset contains the MRI scans of 369 patients, and the validation dataset has MRI scans of 125 patients. The detailed description of the dataset is given in Chapter 3, section 3.2.1. (Menze et al., 2015; Bakas et al., 2017b; a, 2019; Bakas, Spyridon; Akbari, Hamed; Sotiras, Aristeidis; Bilello, Michel; Rozycki, Martin; Kirby, Justin; Freymann, John; Farahani, Keyvan; Davatzikos, 2017)

1.2 Problem Statement

The early and correct diagnosis of brain tumours gliomas plays an important role in improved and timely treatment of brain tumour patients to increase their survival rate. MRI is the most popular non-invasive technique used for diagnosis and monitoring of treatment of glioma patients. The manual brain tumour segmentation done from MRI images gives a low level of accuracy and it is a time-consuming task for a physician. Finding a fully automated model for accurately segmenting the brain tumours would help the doctors in better diagnosis, the assessment of tumour progression, treatment planning, and follow-up. It would also save time. It helps the patients to get timely and proper treatment as it is very important for the patients suffering from high-grade gliomas (HGG) to get required treatment on time. But as gliomas are inherently heterogeneous (in shape, appearance, and histology), it is a very challenging task to accurately segment gliomas in multimodal MRI brain scans. So, it becomes extremely important to find the best state-of-the-art model to automatically segment brain tumours in MRI scans with improved accuracy for better diagnosis and treatment.

1.3 Research Questions

Can any improvement in the automatic segmentation of the glioma sub-regions be achieved by using state-of-the-art architectures in neural networks ?

1.4 Aim and Objectives

The main aim of this research is to propose a model for the automatic segmentation of glioma sub-regions. The automatic segmentation of glioma sub-regions in the brain images is of great importance as it helps in easy, quick, and better diagnosis, giving required treatment in time,

assessment of tumour progression before and after treatment, and also to check the success of the treatment strategy.

The research objectives formulated based on the aim of this study are as follows:

1. To analyze the multimodal MRI brain scans to understand the modalities of the scans and the various sub-regions of the tumours.
2. To analyze various state-of-the-art architectures that can be used for automatic segmentation of the glioma sub-regions.
3. To identify a most suitable architecture for automatic segmentation of glioma sub-regions
4. To assess the model performance based on the model evaluation metrics.

1.5 Significance of this study

This study helps in finding if the brain tumour, gliomas, and its sub-regions can be segmented with improved accuracy. Finding a fully automated model for accurately segmenting the brain tumours would help the neurologists and neurosurgeons for better diagnosis, in the assessment of tumour progression, in treatment planning, and follow-up. It would also save doctors time. It also helps the patients to get timely and proper treatment as it is very important for the patients suffering from high-grade gliomas (HGG) to get required treatment on time.

1.6 Scope of this study

As part of this work, the performance of the CGAN with U-Net as the generator for segmentation of glioma sub-regions will be studied. The other state-of-the-art architectures are out of the scope of this research. This research will be done on the BraTS 2020 challenge data set. It includes brain images of 369 patients as the training data set and brain images of 125 patients as the validation data set. Brain images from any other source are not included in this study.

1.7 Structure of the study

The structure of the thesis is as follows:

In Chapter 1, Section 1.1 presents the background of the research on brain tumour segmentation. Section 1.2 states the problem that is being addressed as part of this research. Section 1.3 contains the research questions that would be answered as part of this research. Section 1.4 discusses the aim and objectives of the research. Section 1.5 presents the

significance of this study. Section 1.6 gives the scope of this study. Finally, section 1.7 describes the structure of this thesis.

Chapter 2 presents the necessary theoretical background and the work done in similar research areas. Section 2.1 gives a brief description of what is covered in chapter 2.Section 2.2 presents information on brain anatomy, type of brain tumours, risk factors, symptoms, methods to diagnose the brain tumours and treatment. Section 2.3 discusses the data formats used for storing medical images. Section 2.4 presents the work done on the evaluation metrics used for assessing models for the quality of segmentation. Section 2.5 discusses various methods and architectures used for segmentation of images, biomedical image segmentation. Section 2.6 presents the top-ranking models in BraTS challenge from BraTS 2012 to 2019. Finally, section 2.7 discusses the surveys conducted on the BraTS challenges and the conclusions drawn from the surveys.

Chapter 3 discusses the methodology to be used in the research. Section 3.1 gives an introduction to chapter3. Section 3.2 describes the research approach that would be used to address the research problem. It explains the various steps involved like data selection, data pre-processing, data transformation, evaluation of the model. Section 3.3 describes the details of the proposed model for achieving the aims and objectives of the research. Finally, section 3.5 presents a summary of the chapter.

CHAPTER 2

LITERATURE REVIEW

2.1 Introduction

This chapter focuses on explaining the previous works done on automatic segmentation of brain tumour glioma sub-regions. This section summarizes the literature beginning with brain anatomy and types of brain tumours, risk factors, symptoms, tests conducted for diagnosing brain tumours and treatment. It explains the formats in which brain images are stored and how they are interpreted. It then summarizes the analysis on the metrics used for evaluating the models for segmentation of brain tumours. It is followed by a summary on different models and architectures that showed great performance in past for segmentation of images. Then it shows the evolution of methods used for segmentation of glioma sub-regions by discussing the top-ranking methods in the BraTS challenge from 2012 to 2019. Finally summarizes the different benchmarks and surveys, conducted on the BraTS challenge.

2.2 Brain Tumours

2.2.1 Brain Anatomy and Types of Tumours

The brain and the spinal cord constitutes the central nervous system. The brain is made up of various kinds of cells. The most prevalent among them are the neurons and the glial cells.

- Neurons transmit signals from the brain to the spinal cord and the body, and they also receive the signals from the rest of the body to the brain. There are more than a trillion neurons in the human brain.
- Glial cells insulate, feed and provide structural support to neurons. They also help in disposing the dead neurons. Glial cells are of different types each with specific functionality. Astrocytes, oligodendrocytes, and ependymal cells are the types of glial cells.

Brain tumour refers to a collection of neoplasms, each with specific biology, prognosis, and treatment. A neoplasm is an abnormal growth of cells also known as a tumour. Brain tumours are classified into primary and secondary. The malignant tumours that form in the brain or in the nerves originating in the brain are the primary brain tumours. The malignant tumours that originate elsewhere and metastasize to the brain are the secondary brain tumours. The primary brain tumours are further classified into gliomas and non-gliomas.

- Gliomas: The malignant primary brain tumours that originate in the glial cells of the central nervous system are gliomas..
- Non-Gliomas: These brain tumours that do not arise from glial cells. (Arevalo et al., n.d.; Wen and Kesari, 2008; Louis et al., 2016; Brain Cancer | CancerQuest, 2020)

2.2.2 Risk Factors

The cause for the majority of malignant gliomas has been unidentified. However, the below factors have been identified as possible risk factors.

- Genetic disorders
- Age (Exception the tumors commonly occuring in young children).
- Head injuries
- Consumption of N-nitroso compounds during pregnancy might lead to an increased risk of brain tumour in offsprings(Arevalo et al., n.d.; Wen and Kesari, 2008; Louis et al., 2016; Brain Cancer | CancerQuest, 2020).

2.2.3 Symptoms

Patients with gliomas can suffer from various symptoms like headaches can be with nausea, vomiting, seizures, problems with specific nerve functions, confusion, and memory loss and personality changes (Arevalo et al., n.d.; Wen and Kesari, 2008; Louis et al., 2016; Brain Cancer | CancerQuest, 2020).

2.2.4 Diagnosis

The following tests are usually conducted for diagnosing brain tumours

- Neurological exam
- Cerebral angiography
- CT Scan
- MRI Scan
- Surgical biopsy (Arevalo et al., n.d.; Wen and Kesari, 2008; Louis et al., 2016; Brain Cancer | CancerQuest, 2020).

2.2.5 Treatment

Treatments differ based on various factors, like the patient's age, patient's health conditions, cancer stage, tumour's location, the aggressiveness of the tumour and more.HGG patients need immediate and aggressive treatment whereas the treatment of patients with LGG is

delayed as they can survive for several years. Treatments can include surgery, radiation therapy, chemotherapy, resection, and ancillary therapeutic agents (Arevalo et al., n.d.; Wen and Kesari, 2008; Louis et al., 2016; Brain Cancer | CancerQuest, 2020).

2.3 Data Format

The medical images are the depiction of the internal structure of organs as an array of pixels or voxels. The numerical value of the pixel or the pixel data is based on the acquisition protocol, the imaging modality, the post-processing and the reconstruction.

The photometric interpretation of an image describes how the pixel data (the numerical value of pixels) should be interpreted correctly as a monochrome or colour image. The number of channels or samples per pixel is used to specify colour information in the image pixel values. Monochrome images use shades of grey from black to white with one sample per pixel or to show the images. The number of shades of grey depends on the number of bits used to represent the information of each pixel which is called pixel depth. The medical images, like x-rays, CT and MRI scans which are used for diagnosis have a greyscale photometric interpretation.

Metadata, the information that describes the image is usually stored at the start of the file as a header and contains information like the photometric interpretation, image matrix dimensions, the pixel depth, and the spatial resolution. Metadata plays an important role in the case of medical images, as the images from diagnostic modalities usually have the information on how the image was generated. For example, an MRI image contains parameters related to the pulse sequence used, e.g., the number of acquisitions, flip angle, timing information etc. Pixel data contain the numerical values of the pixels.

Medical image files are usually stored in two configurations. The first configuration contains both the metadata and image data, with the metadata stored at the start of the file. Dicom, Minc, NIfTI etc. file formats use this. The second configuration stores the image data and the metadata in two separate files. The Analyze file format uses the second configuration.

NIfTI is a file format that was created for neuroimaging by a committee based at the National Institutes of Health at the beginning of 2000s.NIfTI file format also allows the storage of the pixel data and header in separate files. The header and pixel data are merged and saved as a single ".nii" file. NIfTI supports different data types which allow minimizing or eliminating

the use of scale factor. The table below gives the details of the NIfTI file format (Larobina and Murino, n.d.).

Table 2.1: Details of NIfTI file format

Format	Header	Extension	Data types
NIfTI	Fixed-length: 352 byte binary format(348 byte in the case of data stored as .img and .hdr)	.nii	Signed and unsigned integer (from 8- to 64-bit), float (from 32- to 128-bit), complex (from 64- to 256-bit)

2.4 Evaluation Metrics

Medical Image segmentation is an important step in image processing. Evaluating the quality of segmentation plays a crucial part in measuring the progress in this research area. Segmentation methods with high accuracy are very important in planning surgeries. Abdel Aziz Taha* and Allan Hanbury (Taha and Hanbury, 2015b) proposed an efficient evaluation tool for segmentation of 3D medical images using 20 evaluation metrics. This tool provides a set of metrics as a standard for evaluating medical image segmentation. This tool is implemented in the project "EvaluateSegmentation. This tool uses efficient techniques to achieve efficienct speed, memory and to overcome the challenges in the evaluation of medical segmentations like evaluating images with large grid size. As the metrics have different properties, choosing the suitable metrics is an important task. This paper provides an analysis of the 20 metrics, specific to their properties, and appropriateness to evaluate segmentation, based on specific requirements and segmentations with specific properties. This paper provides guidelines for selecting the metrics that are suitable based on the data, the segmentation task and other requirements.

2.5 Image Segmentation

Jonathan Long et al. (Long et al., n.d.) proposed that when FCNs are trained to end-to-end, pixel to pixel shows good performance in semantic segmentation of images. The main idea was to build fully convolutional networks that take input of the random size and generate output that is correspondingly sized as input with efficient inference and learning The authors adapted contemporary networks for classification AlexNet (Krizhevsky et al., 2017), the VGG net(Simonyan and Zisserman, 2015), and GoogLeNet (Szegedy et al., n.d.) into fully convolutional networks and transferred the representations learned by fine-tuning to the segmentation task. They defined a skip architecture that combines deep, semantic, coarse

information and shallow, fine, appearance information to produce accurate and detailed segmentations. The model showed good performance in segmentation of PASCAL VOC (20% relative improvement to 62.2% mean IOU on 2012), NYUDv2, and SIFT Flow. The model showed 20% improvement in the performance compared to the contemporary models on the PASCAL VOC 2011 and 2012 test sets and also reduced inference time.

Semantic segmentation predicts a category label for each pixel in the input image. Pauline Luc et al. (Luc et al., n.d.) proposed an adversarial approach for training the semantic segmentation models. A convolutional network for semantic segmentation is trained along with an adversarial network to discriminate between ground truth segmentation maps and the segmentation maps produced by the segmentation network. Their work has the following advantages compared to previous approaches: (i) the high capacity of the adversarial model make it flexible to detect mismatches between the model predictions and the ground-truth, without manually defining these. (ii) The model trained once performs efficiently as it does not involve any higher-order terms or recurrence. Experiments were conducted using this model on Stanford Background and PASCAL VOC 2012 datasets. This approach showed improvement compared to standard models with an accuracy of 68.7(per class) 75.2(pixel) 54.3 (Mean IOU) on the Stanford Background data set. The model achieved a mean IOU of 73.1 for the baseline model, 73.3 for LargeFOV-Product and 73.2 LargeFOV-Scaling on the PASCAL VOC 2012 test set.

Olaf Ronneberger et al. (Ronneberger et al., 2015) proposed a network and strategy for training that is based on data augmentation for efficient use of available annotated data. The FCNS were modified and extended (Long et al., n.d.) in such a way that it can be trained with very few images but can result in more accurate segmentation. The architecture proposed in this paper consists of a contracting and an expanding path. The pooling operators are replaced with upsampling operators to increase the resolution of the output. Upsampling results in more number of feature channels, allowing the network to pass on the context information to higher resolution layers. The path that is expansive is almost symmetrical to the path that is contracting, and results in a u-shaped architecture. Contracting path resembles a CNN and captures the context. The expanding path is used for precise localization. They showed that model can perform better compared to the prior models when trained end-to-end even from a very few samples. The model was applied for the segmentation in EM segmentation challenge and for cell segmentation task in ISBI cell tracking challenge. The u-

net architecture has shown outstanding performance on different biomedical segmentation tasks. The model achieved an average IOU of 92%.On the second data set DIC-HeLa the model achieved an average IOU of 77.5% .

Fausto Milletari et al. (Milletari et al., 2016) proposed an approach for segmentation of 3D images based on a volumetric FCN. Unlike other approaches, volumetric convolutions instead were used instead of processing the input volumes slice-wise. An objective function based on Dice coefficient maximisation was optimized during training. The model comprises of compression path on the left which compresses the input while and a decompression path on the right which decompresses the signal to its original size. This architecture converges in a fraction of the time needed by a similar network that does not learn residual functions. PReLu non-linear activation functions are applied throughout the network. The model was trained end-to-end on 50 prostate MRI scans PROMISE2012 challenge dataset. The model achieved an average Dice score of 0.869 ± 0.033 when tested on 30 MRI scans from PROMISE2012 challenge dataset. It was concluded that future works would aim at the segmentation of volumes containing multiple regions in other modalities like ultrasound and at higher resolutions by splitting the network over multiple GPUs.

Vivek Kumar Singh et al.(Singh et al., 2018) proposed an approach for breast mass segmentation in mammography based on CGAN. The generator part of the CGAN is used in the first stage to obtain a binary mask that selects the pixels that represent the area of the breast mass and ignores the pixels that represent the healthy tissue. The mammogram cropped to contain the mass ROI. The image was regularized with a Gaussian filter for noise removal. The second stage contains a CNN to classify the binary mask obtained in the first stage into one of the 4 classes of mass shape (round, oval, lobular, and irregular). Experiments were performed on DDSM dataset. Their model achieved very high Dice coefficient and Jaccard index (> 94% and > 89%, respectively). Furthermore, to detect portray significant morphological features of the segmented tumour, a specific CNN was designed for classification of the segmented tumour areas into four types (irregular, lobular, oval and round), with an overall accuracy of about 72%.

2.6 Brain Tumour Segmentation

Sérgio Pereira et al (Pereira et al., 2016) proposed an automatic segmentation method based on CNNs, using small 3x3 kernels. The use of small kernels helped in designing a deeper

architecture, and also in overcoming the problem of overfitting, with the fewer number of weights in the network. It was investigated that the use of intensity normalization as a pre-processing step together with data augmentation demonstrated to be very effective for brain tumour segmentation in MRI images. It was verified that the LReLU (Maas et al., 2013) activation function was more effective compared to ReLU activation function in training the CNN. This proposal was validated on the BraTS 2013 (Training set containing 20 HGG and 10 LGG cases. The Leaderboard set containing 21 HGG and 4 LGG cases. The Challenge set containing 10 HGG cases) and BraTS 2015 (Training set containing 220 and 54 HGG and LGG cases, respectively. The Challenge set containing 53 cases, including both grades) data sets. The computation time was reduced approximately by ten-fold. The model could perform well on HGG cases compared to LGG cases. The proposed model could achieve the below results on BraTS 2013 and BraTS 2015 data set.

Table 2.2: Results obtained by the model proposed by Sérgio Pereira et al. on BraTS 2013 and BraTS 2015 data sets

Data Set	Complete	Core	Enhancing
BraTS 2013	0.88	0.83	0.77
BraTS 2015	0.78	0.65	0.75

Table 2.3: Results obtained by the model proposed by Sérgio Pereira et al. on BraTS 2013 leader board dataset

Grade	Complete	Core	Enhancing
HGG	0.88	0.77	0.73
LGG	0.65	0.53	0.00
Combined (HGG+LGG)	0.84	0.72	0.62

Mina Rezaei et al. (Rezaei et al., n.d.) proposed an architecture which can be trained from end-to-end for brain tumour segmentation using CGAN. A CNN for semantic segmentation is trained along with an adversarial network for discriminating between segmentation maps from the ground truth and segmentation maps from the segmentation network. The model used U-Net (Ronneberger et al., 2015) as the generator and Markovian GAN (Li and Wand,

n.d.) as the discriminator. Virtual-BatchNorm convolution (Openai, n.d.) was used in the generator network and Reference-BatchNorm (Openai, n.d.) was used in the discriminator network to reduce over-fitting. The adversarial training also helped in reducing the over-fitting and increasing the robustness of the model. This model was validated on brain images from BraTS 2017 containing the brain images of 75 LGG and 210 HGG cases. The proposed model achieved on a Dice score, Sensitivity and Specificity of 0.68, 0.99 and 0.98 respectively for the whole tumour. It was suggested that further improvement could be achieved on the generative network by using a RNN inside the Encoder-Decoder.

Table 2.4: Results obtained by the model proposed by Mina Rezaei et al. on BraTS 2017 data set

	Whole Tumour	**Tumour Core**	**Enhanced Tumour**
Dice Score	0.70	0.55	0.40
Sensitivity	0.68	0.52	0.99
Specificity	0.99	0.99	0.99

Hao Dong et al. (Dong et al., 2011) proposed a U-Net based deep convolutional networks for automatic segmentation of brain tumours. An extensive data augmentation scheme containing rigid deformation, a transformation that is brightness and elastic distortion based has been coupled with the U-Net that comprises of skip-architecture. The model was validated on the BraTS 2015 dataset containing 220 HGG and 54 LGG cases. This method could not show good performance on segmentation of enhancing tumour of the LGG cases in T1c images due to the following reasons: (I) in most of the LGG cases blood-brain barrier remains intact and the tumour regions are not often contrast-enhanced; (II) the dataset contains only 54 LGG cases which might be insufficient for training the model and (III) the borders between enhanced tumour and non-enhanced regions in the LGG cases are more spread out and less visible which makes it challenging for segmentation. It was suggested that it might be possible to solve this problem by stacking the multimodal channels of MRI images and performing training jointly with HGG datasets. Despite the above limitations, the proposed model could achieve the below Dice Scores.

Table 2.5: Results obtained by the model proposed by Hao Dong et al. on BraTS 2015 data set

Grade	Complete	Core	Enhancing
HGG	0.88	0.87	0.81
LGG	0.84	0.85	0.00
Combined(HGG+LGG)	0.86	0.86	0.65

Shaoguo Cui et al proposed (Cui et al., 2018) an approach that not only localizes the entire tumour region but also accurately segments the intratumor regions. The proposed work was used a cascaded deep learning CNN comprising of two subnetworks: (I) a TLN and (II) an ITCN. A modified FCN (Long et al., n.d.) in conjunction with the transfer learning technology was used as the TLN to process MRI brain images and to define the tumour. Influenced by the model proposed by Simonyan and Zisserman (Simonyan and Zisserman, 2015) a CNN with deeper architecture and smaller kernel was used as the ITCN to classify the defined tumour region into multiple sub-regions. The TLN subnetwork requires only a forward computation to localize the whole tumour region as the first step. Then, the ITCN subnetwork only needs to classify the much-reduced region defined by the TLN into different subregions. This helped in improving the efficiency of computing. The model has been validated on BraTS 2015 dataset. The proposed model was able to complete a segmentation task within 1.54 seconds. It was suggested that in the future, deep learning neural networks could be extended to include histological and other important data for improving the clinical management of brain tumours. The model achieved the below results on BraTS 2015 dataset.

Table 2.6: Results obtained by the model proposed by Shaoguo Cui et al. on the BraTS 2015 data set

Grade	Complete	Core	Enhancing
HGG	0.90	0.81	0.81
Combined(HGG+LGG)	0.89	0.77	0.8

Despite addressing the class imbalance problem and showing excellent performance, model cascade (MC) strategy ignores the correlation among the models and leads to unwanted system complexity. Chenhong Zhou et al.(Zhou et al., 2020) proposed a light-weight deep

model OM-Net to address class imbalance problem in a better way compared to MC strategy. It needs only one-pass computation for segmentation of brain tumours. In the end, a simple yet effective post-processing method was used to refine the segmentation results. The model was validated on BraTS 2015, BraTS 2017 and BraTS 2018 datasets. Despite having only one-third of the parameters of MC, OM-Net shows better performance in segmentation of brain tumours and its sub-regions, specifically on the tumour core and enhancing tumour. It was observed that the OM-Net^p performed better when compared to OM-Net and OM-Net + CGAp (OM-Net + CGA with post-processing) performed better when compared with OM-Net + CGA showing that post-processing operation improves for the complete tumour and tumour core regions. The below results were achieved by OM-Net + CGA^p on BraTS 2015, BraTS 2017 and BraTS 2018 datasets.

Table 2.7: Results achieved by OM-Net + CGA^p proposed by Chenhong Zhou et al. on BraTS 2015,BraTS 2017 and BraTS 2018 datasets

	Complete	**Core**	**Enhancing**
BraTS 2015	0.8700	0.7500	0.6500
BraTS 2017	0.9071	0.8422	0.7852
BraTS 2018	0.9078	0.8575	0.8111

Mohammad Havaei et al. (Havaei et al., n.d.) presented a novel two-pathway CNN architecture which exploits both local features of the brain and more global contextual features simultaneously.A 2-phase training procedure to tackle problems due to the imbalance of tumour labels was proposed. A cascaded architecture in which the output of a basic CNN is given as an additional source of information for a subsequent CNN. To train a cascaded architecture, TwoPathCNN was trained with the two-phase stochastic gradient descent procedure and then, the parameters of the TwoPathCNN were fixed and included in the cascaded architecture and then the remaining parameters were trained using a similar procedure The proposed method takes between 25 seconds and 3 minutes for segmentation, which is one order of magnitude (over 30 times) faster than the contemporary methods. The model was evaluated on BraTS 2013 dataset. The below results were achieved on the BraTS 2013 test data set.

Table 2.8: Results obtained by Mohammad Havaeia et al. on BraTS 2013 test data set

	Complete	Core	Enhancing
InputCascadeCNN*	0.88	0.79	0.73
MFCascadeCNN*	0.86	0.77	0.73
TwoPathCNN*	0.85	0.78	0.73
LocalCascadeCNN*	0.88	0.76	0.72
LocalPathCNN*	0.85	0.74	0.71

2.7 Benchmarks & Surveys

In (Liu et al., 2014) Jin Liu, Min Li provided a broad overview of methods used for brain tumour segmentation in MRI images. This paper classified the brain tumour segmentation methods into three important categories: conventional methods, classification and clustering methods, and deformable model methods. Conventional brain tumour segmentation methods mainly include threshold-based methods and region-based methods which are the standard methods for image processing. The following classification or clustering methods are discussed in this paper: Fuzzy C-Means (FCM), k-means, Markov Random Fields (MRF), Bayes, Artificial Neural Networks (ANN), Support Vector Machines (SVM), Atlas-based, etc. In this section, FCM, Atlas-based, MRF, and SVM for segmenting brain tumour. The deformable models are further classified into Parametric deformable models and Geometric deformable models. It was concluded that due to a lack of interaction between researchers and clinicians, clinicians still rely on manual segmentation for the brain tumour in many cases. Therefore, it will be useful if the tools developed are placed in more user-friendly environments. It was also concluded that computation, robustness are also important criteria for assessing the models. It was suggested that the feature extraction for brain tumour would help in looking at relevant and meaningful features designing new features to obtain improved results. This would help in improving the accuracy, validity, and robustness of brain tumour segmentation of MRI images.

Bjoern H. Menze et al(Menze et al., 2015) analyzed and reported the results of BraTS 2012 and 2013. Segmentation algorithms were expermineted on a set of 65 multi-contrast MRI scans of LGG and HGG patients which were manually annotated and to 65 synthetic scans generated using tumour image simulation software. The algorithms could reach Dice scores of over 80% for the whole tumour, 70% tumour core region and 60% for active core region

segmentation. Segmentation of the tumour core region and specifically the active core region in HGG was challenging. It was found that different algorithms performed best for segmentation of different glioma sub-regions and no single algorithm showed the best performance in segmentation of the entire tumour regions considered. It was also found that fusing the best performing algorithms using a hierarchical majority vote or by other fusion, strategies resulted in segmentations that consistently performed better than all individual algorithms. It was inferred that apart from pushing the limits of individual algorithms, the best performance can be achieved by fusing several best performing individual. This observation is in agreement with the concept from ensemble learning, when a set of predictors those are unbiased but with high variability in the individual prediction, improve when their predictions are pooled. Optimization of the ensemble prediction can be done by fusing many predictors for balancing variability reduction and fuse only a few selected predictors for bias removal. It was also proposed that the best performing algorithms relied on a discriminative learning approach. The other methods that used image intensities and standard normalization algorithms also performed well. The spatial processing which takes into account the information about tumour structure at a regional "super-voxel" level showed exceptional performance for "whole" tumour and tumour "core".

Spyridon Bakas et al. (Bakas et al., 2019) assessed the ML methods used for brain tumour image segmentation in MRI scans of BraTS challenge from 2012-2018. They investigated the challenge to identify the best machine learning algorithms for segmentation of brain tumour and its sub-regions. It was observed that despite an excellent performance by the individual automated segmentation methods, they could not exceed the performance of the inter-rater agreement, across expert clinicians. It was found that the fusing the segmentation labels from top-ranked algorithms showed better performance when compared with all individual methods and was comparable to the inter-rater agreement. It was suggested that ensembling of segmentation algorithms that were fused might be the favoured approach for translation of tumour segmentation methods into clinical practice. Despite improved accuracy, the robustness of individual automated segmentation methods was still below the level of inter-rater agreement. This robustness was expected to improve with the increase in the training set size which captures diversified patient populations, in addition to improved training strategies and ML architectures. The strategies to ensemble several models decrease the outliers and increase the precision of automated segmentation systems, using harmony in segmentation across different models. It was suggested that future research is necessary, to increase the

robustness of individual approaches by improving the ability of segmentation systems to handle effects that are confounding which are seen in images obtained using routine clinical workflows, to improve performance in segmentation of LGG, featuring scattered boundaries, especially in cases without active tumour sub-regions and to detect and evaluate their slow progression effectively.

Mina Ghaffari et al.(Ghaffari et al., 2020) analyzed the evolution of models for automatic segmentation of multimodal MR brain tumour images. The top-ranked 12 models in BraTS from 2012-2018 and some of the models that performed well on the BraTS dataset and external to the challenge were explained in detail. This study indicated that the top-performing models in the initial stages of the BraTS used Random Forests (BraTS 2012-2014), while most of the submissions to BraTS 2015-2018 used deep learning. Deep learning models more specifically, CNN-based models showed outperformed the other models for the segmentation task. Recent advancements in deep learning models like batch normalization, non-linear activation and drop out improved the accuracy of these models. 3D CNNs produced higher accuracy but the GPU memory available for training a model could be the limiting factor. To overcome this, models were trained using 2D slices extracted from different views of MRI images and then the prediction of all CNN are fused to achieve the final segmentation result with improved accuracy (Zhao et al., 2018), (Chandra et al., 2019). Another way to compensate for the limited GPU memory is by training the CNN using patches extracted from images. The main problem of patch-wise approach is small patches can only consider the local image information and do not take into account the context related information on a larger scale. To overcome this issue multi-scale training was proposed (Kamnitsas et al., n.d.) (Havaei et al., 2016). Modern GPUs having large memory sizes reduced a few of these problems. CNNs were trained using large 3D patches (Isensee et al., 2018a) (Chen et al., 2019), or even on whole images (Myronenko, 2019) which resulted in considerably high Dice scores. To enhance the performance even further, CNN models were modified which resulted in networks such as ResNet and DenseNet. The model that used these architectures reported enhancement in Dice score accuracies (Kamnitsas et al., n.d.), (Chen et al., 2019),(Myronenko, 2019). Models using U-net have outperformed most of the other CNN-based segmentation models. Isensee et.al showed that “a well-trained U-net is hard to beat”(Isensee et al., n.d.) with their U-net models in BraTS18 and BraTS17. Their success indicated that the non-architectural aspects of a segmentation method like including appropriate pre-and postprocessing steps, hyperparameters tuning, and application of

ensembling can influence its result significantly(Isensee et al., 2018b). It was found that ensembling enhances the robustness of a model and improves model accuracy. The ensemble of best performing models were evaluated and it was noticed that fusion of segmentation labels compare to all other models in segmenting all tumour subregions (Bakas et al., 2019). The top-ranked models in BraTS 2018 used ensembling. Due to the efforts in the BraTS, it was possible to achieve Dice score of more than 0.90 for the whole tumour segmentation. It was suggested that the improvement could be achieved by using various techniques for processing images, changing the deep learning models, and increasing the size of the dataset. The following Figure 2.1 shows the graph of the segmentation accuracies achieved by top-performing models of BraTS challenges from 2012-2018.

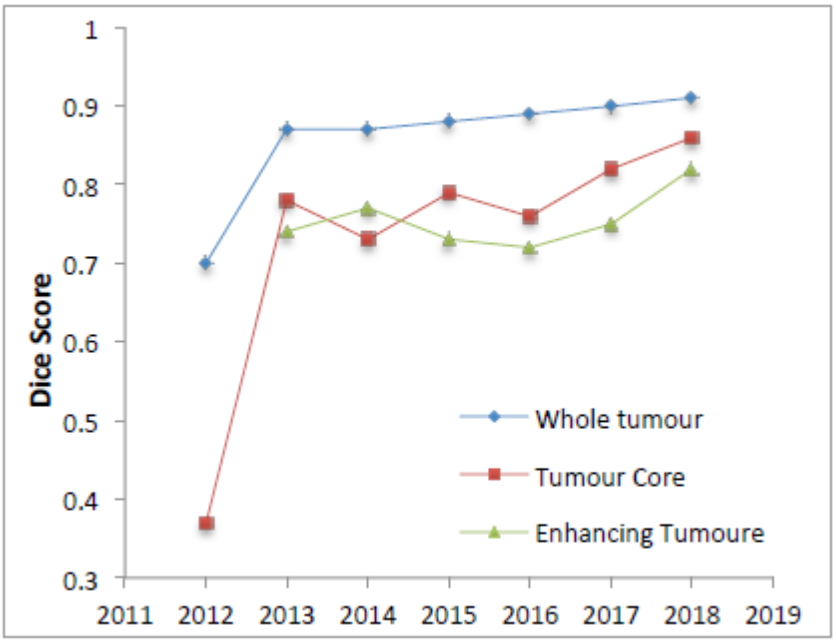

Figure 2.1: The graph of segmentation accuracies achieved by top-performing models of BraTS challenge from 2012-2018

The summary of the methods used by top-ranking models in BraTS from the year 2012 to 2019 is presented in section appendix c.

2.8 Discussion

By analyzing the previous works done on the brain tumour segmentation the following important points were observed: The feature extraction for brain tumour would help in looking at relevant and meaningful features and designing new features to obtain improved results. The computation time and robustness are also important criteria for assessing the

segmentation models apart from the accuracy of the segmentation. The robustness can be improved by increasing the size of training so that it captures more diversified patient populations, also by improved training strategies and machine learning architectures. The computation time can be reduced by using modern GPUs.

Different algorithms performed best for segmentation of different glioma sub-regions and no single algorithm showed the best performance in segmentation of the entire tumour regions considered. Fusing the best-performing algorithms using a hierarchical majority vote or by other fusion, strategies resulted in segmentations that consistently performed better than all individual algorithms. It was inferred that in addition to pushing the limits of individual algorithms, the best performance can be achieved by fusing several best performing individual. It was found that ensembling enhances the robustness and the accuracy of the model.

It was observed that the best performing algorithms were based on a discriminative learning approach. The other methods that used image intensities and standard normalization algorithms also performed well. The spatial processing which considers information about tumour structure at a regional “super-voxel” level, did exceptionally well for “whole” tumour and tumour “core”. A good understanding of the image resolution and image subsampling help in improving speed and segmentation quality.

Automatic brain tumour segmentation is not still widely used due to a lack of interaction between researchers and clinicians. Therefore, it will be more useful if the tools developed are placed in more user-friendly environments. Future research is necessary, to improve the robustness of individual approaches by enhancing the ability of segmentation systems to handle effects that are confounding which are seen in images obtained using routine clinical workflows.

2.9 Summary

This chapter presents an understanding of brain anatomy, type of brain tumours, risk factors, symptoms, methods to diagnose the brain tumours and treatment. It gives information on the data formats used for storing the medical images. It presents the work done on the evaluation metrics used for assessing models for the quality of segmentation. It discusses various methods and architectures used for segmentation of images and biomedical image segmentation. It analyses the top-ranking models used in BraTS challenge from the year 2012

to 2019. It presents conclusions and suggestions given in the benchmarks and surveys conducted on the BraTS challenges. Finally, it discusses the conclusions, the suggestions, the gaps and the inferences drawn during the analysis of the previous works on brain tumour segmentation.

CHAPTER 3

RESEARCH METHODOLOGY

3.1 Introduction

This chapter starts with explaining the process followed in this research. It describes the various steps involved in the research process. It is followed by the approach used in the research. The research approach discusses the details of the dataset and its selection. The data transformation techniques used for converting the MRI brain images which are in nifty format to the format needed for the segmentation task. The pre-processing techniques used for processing the input data before feeding it into the deep learning network. The data augmentation techniques used to increase the amount of data by slightly modifying the existing data so that the model can be trained well. The metrics used for evaluating the performance of the model. Finally, it describes the proposed architecture and the method for the segmentation of the brain tumours and its sub-regions.

3.2 Research Process

The following figure presents the flow chart that shows the process followed in this research. The research process starts with the search of existing literature on the chosen topic automatic brain tumour segmentation. It is followed by the review of the existing literature to gain an understanding of the existing research, to analyze the existing methodologies and architectures, to know the latest advancements happened, to find the research gaps on automatic brain tumour segmentation. After the literature review, the existing artificial neural networks for automatic brain tumour segmentation are analyzed. Data set for the research is collected and analyzed to check if it suits the research and to design the model for automatic brain tumour segmentation. The collected data is transformed, pre-processed to required format The data is augmented to well train the model. Parallelly the model is designed for the segmentation task. It is followed by building the model and training the model. Once the model is trained it is evaluated using validation/test data set. This evaluation of the model is done based on the metrics Dice score, specificity, sensitivity, and Hausdorff distance. If the results of the evaluation of model are satisfactory the final report is prepared else the model is parameter tuned or rebuilt to improve the performance.

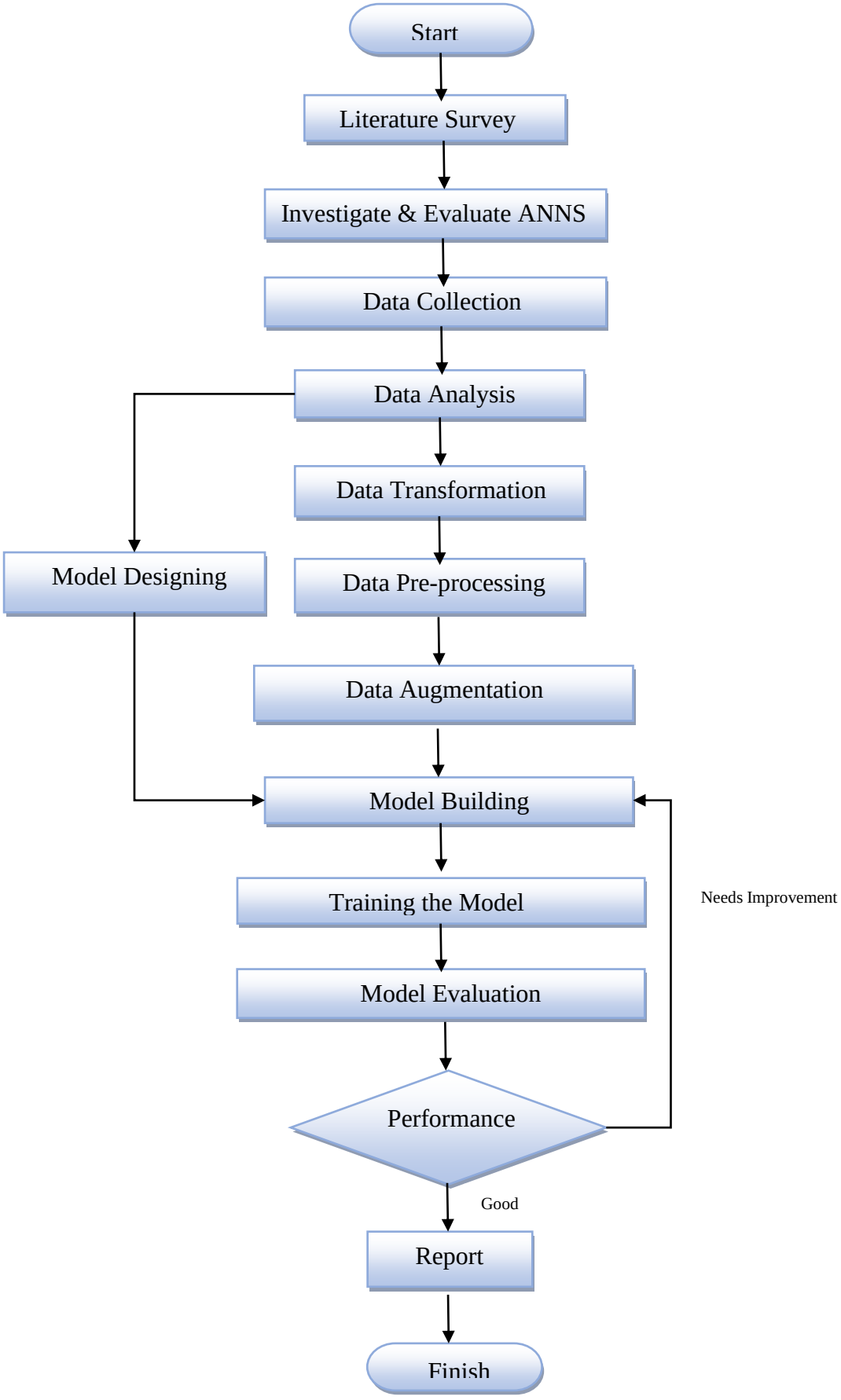

Figure 3.1: Flow chart representing the research process

3.3 Research Approach

The figure depicted below presents the research approach and the model used for the segmentation of brain tumour and its sub-regions. The detail description of each process in the research process is given in the subsequent subsections and sections.

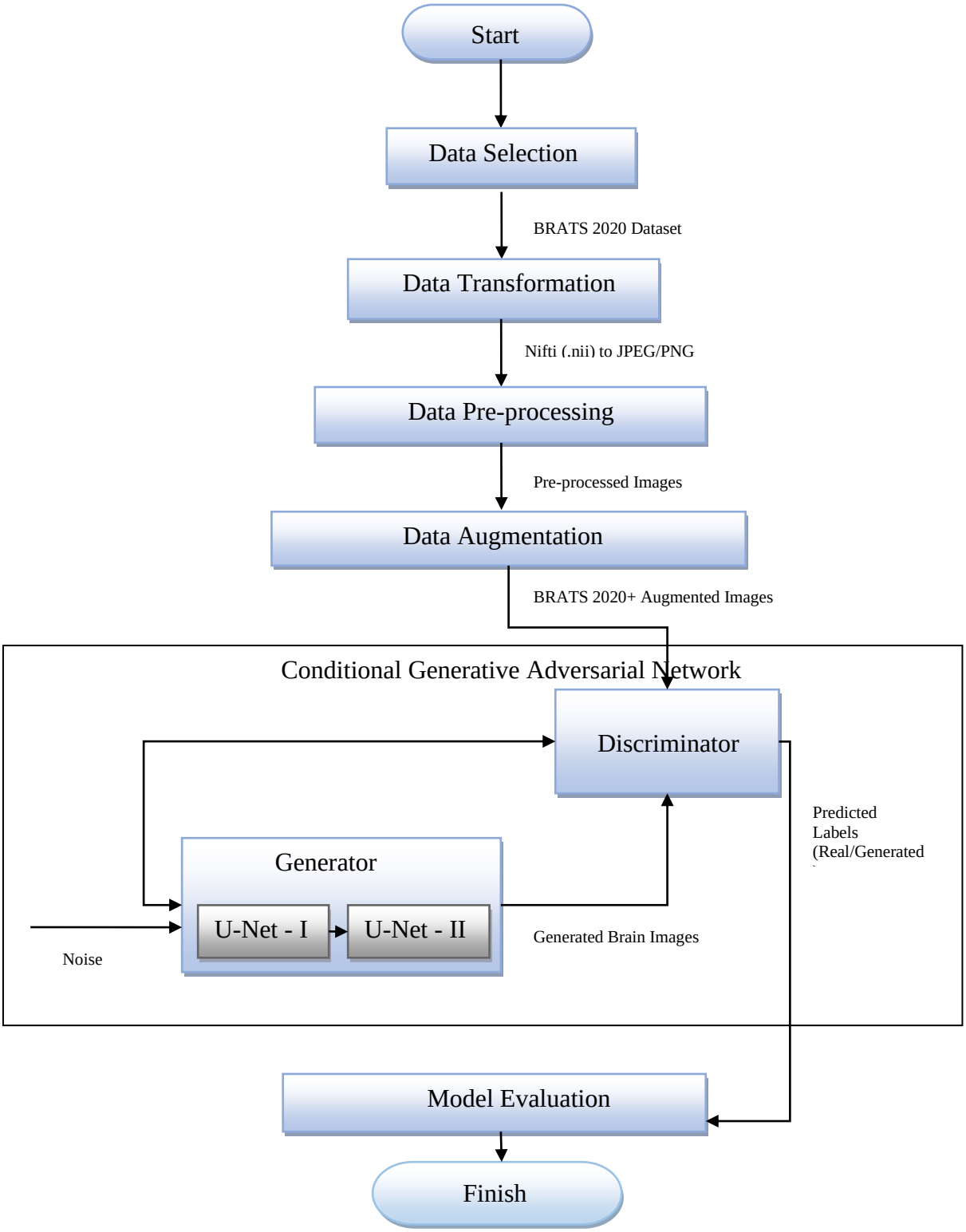

Figure 3.2: Proposed research approach - Model: CGAN with cascaded U-Net as the generator

3.3.1 Data Selection

This research uses the brain MRI scans from BraTS 2020 challenge. The data set contains a training set and a validation set. The training dataset contains the MRI scans of 369 patients, and the validation dataset has MRI scans of 125 patients (Menze et al., 2015; Bakas et al., 2017b; a, 2019; Bakas, Spyridon; Akbari, Hamed; Sotiras, Aristeidis; Bilello, Michel; Rozycki, Martin; Kirby, Justin; Freymann, John; Farahani, Keyvan; Davatzikos, 2017)

The dataset provides the below types of brain images for each patient.

- Native T1 (T1) (T1 images highlight fat tissue within the body)
- Post-contrast T1-weighted (T1-Gd) (Gadolinium is the most commonly used contrast agent for MRI. Abnormal tissue may enhance more than surrounding normal tissue following intravenous gadolinium)
- T2-weighted (T2) (T2 images highlight fat and water within the body) and
- T2 Fluid Attenuated Inversion Recovery (T2-FLAIR) (The signal from a free fluid such as cerebrospinal fluid (CSF) is suppressed on the images)

The figure below (Figure 1) shows the T2 Flair, T1 weighted, T1 post-contrast, and T2 weighted image modalities of the brain.

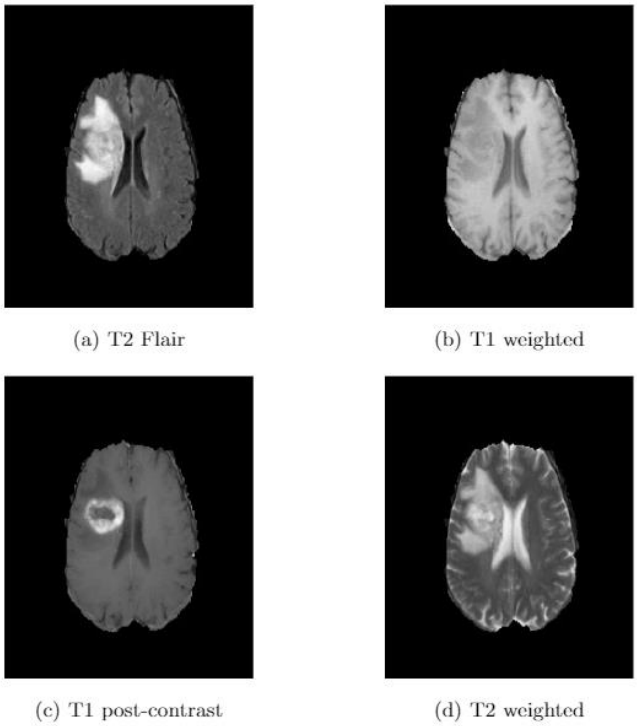

Figure 3.3: Different image modalities of the brain from BraTS dataset(Jiang et al., 2020a)

The figure below (Figure 2) shows the sections of the brain image with glioma sub-regions in different modalities of brain MRI scans. Figure A shows the whole tumour (WT) visible in T2-FLAIR (in yellow). Figure B shows the tumour core (TC) visible in T2 (in orange). Figure C shows the enhancing tumour (ET) visible in T1-Gd (in light blue), that surrounds the cystic/necrotic components of the core (in green). Figure D shows the combination of segmentation along with the labels of glioma sub-regions

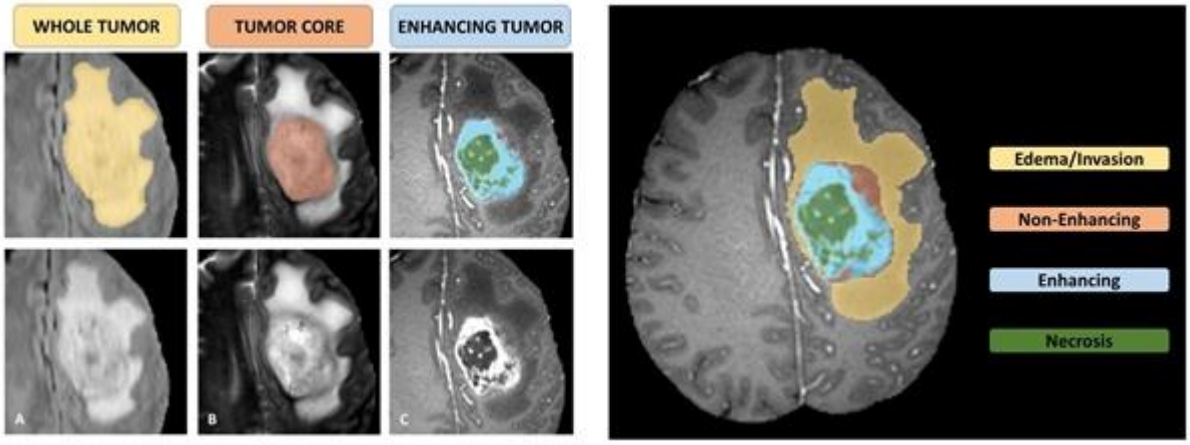

Figure 3.4: Sections of brain images with gliomas sub-regions in different MRI modalities (http://braintumoursegmentation.org/

3.3.2 Data Transformation

The MRI brain scans used in this study are in the NifTI format. These images are converted to png or jpeg format to make the images suitable for further analysis and building the model for segmentation of the brain tumour and its sub-regions. The med2image Python utility converts brain images from NifTI format to png or jpeg format.

3.3.3 Data Pre-Processing

The input data is pre-processed and fed into the neural network, for better results. As the intensity values of the MRI images of the brain are not standardized, the images are intensity normalized by subtracting the mean and dividing by the standard deviation of the intensities of the brain images. Brain MRI scans are monochrome images containing shades of grey from black to white represented as one sample per pixel. Generally, the pixel values are the integers that range between 0 and 255. Feeding the images into the neural network models in their raw format can result in challenges during modelling, like higher computation time than expected

for the training of the model. This can be resolved by scaling the pixel values of the images to the range 0 to 1 before feeding them to the neural network.

3.3.4 Data Augmentation

Training a model on a larger dataset gives better results and prevents overfitting. To add more images to the existing data set the data augmentation technique is used. Different types of data augmentation techniques like flipping the images horizontally and vertically, rotating the images by various angles, scaling the images outward or inward, cropping the image, image translation which involves moving the image along the X or Y direction and adding noise to the images are used to increase the size of the data set.

3.3.5 Evaluation Metrics

The following evaluation metrics are chosen for assessing the model for segmentation of brain tumours in this research(Taha and Hanbury, 2015b):

DICE Coefficient

The Dice coefficient (Dice, n.d.) (DICE), also known as the overlap index, is the most commonly used metric in evaluating medical volume segmentations. Besides the direct comparison between automatic and ground truth segmentations, DICE is commonly used to measure reproducibility (repeatability). Zou et al. (Zou et al., 2004) used the DICE as a measure of the reproducibility as a statistical validation of manual annotation where segmenters repeatedly annotated the same MRI image, then the pair-wise overlap of the repeated segmentations is calculated. A Dice score of 1.0 suggests a perfect segmentation. Dice score can be calculated with the below formula:

$$\mathrm{DICE} = \frac{2\,|\,S_g^1 \cap S_t^1\,|}{|\,S_g^1|\ +\ |\,S_t^1|} = \frac{2\mathrm{TP}}{2\mathrm{TP}\ +\ \mathrm{FP}\ +\ \mathrm{FN}}$$

Equation 3.1: Dice score formula

Sensitivity

True Positive Rate (TPR), also called Sensitivity and Recall, measures the portion of positive voxels in the ground truth that is also identified as positive by the segmentation being evaluated.

$$\text{Sensitivity} = \text{Recall} = \text{TPR} = \frac{\text{TP}}{\text{TP} + \text{FN}}$$

Equation 3.2: Sensitivity formula

Specificity

True Negative Rate (TNR), also called Specificity, measures the portion of negative voxels (background) in the ground truth segmentation that is also identified as negative by the segmentation being evaluated.

$$\text{Specificity} = \text{TNR} = \frac{\text{TN}}{\text{TN} + \text{FP}}$$

Equation 3.3: Specificity formula

Hausdorff Distance

Spatial distance-based metrics are widely used in the evaluation of image segmentation as dissimilarity measures. These metrics are recommended when the segmentation overall accuracy, e.g the boundary delineation (contour), of the segmentation is of importance (Chiu, 2005)Hausdorff distance is one of the distance metrics. The Hausdorff Distance (HD) between two finite point sets A and B is defined by

$$HD(A, B) = \max(h(A, B), h(B,A))$$

Equation 3.4: Hausdorff distance formula

where h(A, B) is called the directed Hausdorff distance and given by:

$$h(A, B) = \max_{a \in A} \min_{b \in B} ||a - b||$$

Equation 3.5: Directed Hausdorff distance formula

where $||a - b||$ is some norm, e.g. Euclidean distance. An algorithm that directly calculates the HD according to the above equation 3.5 takes an execution time of O(|A||B|). Many algorithms calculate the HD with lower complexity. In this paper, we use the algorithm

proposed in (Taha and Hanbury, 2015a)which calculates the HD in nearly-linear time complexity. The HD is generally sensitive to outliers.

3.4 Proposed Model

Inspired by the previous works done on the automatic brain tumour segmentation, proposed an architecture which would use Conditional Generative Adversarial Networks with a cascaded U-Net as the generator. The metrics Hausdorff distance, Dice score, specificity, and sensitivity will be used to evaluate the performance of the model.

The following are the reasons for selecting the above architecture for the segmentation of gliomas sub-regions:

- Gliomas are inherently heterogeneous (in shape, appearance, and histology) in nature. Due to the highly heterogeneous appearance, it is a very challenging task to segment gliomas in multimodal MRI brain scans. The generative network in CGAN learns the intrinsic heterogeneity of gliomas and challenges the adversarial network on its ability to distinguish between real and generated images. The adversarial network in CGAN challenges the generative network by segmenting the tumours accurately. This results in improved performance (Wen and Kesari, 2008) (Mirza and Osindero, 2014).
- U-Net showed excellent performance and is the most widely used architecture in the segmentation of medical images(Ronneberger et al., 2015). The cascaded U-Net architecture showed outstanding performance on brain tumour segmentation(Jiang et al., 2020b)

The model proposed in this paper will use CGAN with a cascaded U-Net as the generative network for the segmentation of gliomas sub-regions.

3.4.1 Conditional Adversarial Networks

In Conditional Generative Adversarial Networks, the generator and discriminator are conditioned on some auxiliary information y, such as class labels or data from other modalities. The generator and discriminator both can be conditioned by feeding them extra information as an additional input layer.

The input noise and labels are presented as input to the generator. The discriminator is fed with real data, generated data, and labels.CGANS use the below minmax loss function as the objective function:

$$\min_{G}\max_{D} V(D,G) = E_{x\sim pdata(x)}[\log D(x|y)] + E_{z\sim pz(z)}\left[\log\left(1 - D\left(G(z|y)\right)\right)\right]$$

Equation 3.6: Minmax loss function used by CGANS

In the above function, D represents discriminator, G represents generator, x represents input data, y represents labels, and z represents noise.

To train a CGAN, both the generative and discriminative networks are trained simultaneously to maximize the performance. The parameters of G(generator) are adjusted to minimize $\log\left(1 - D\left(G(z|y)\right)\right)$ and the parameters of D(discriminator) are adjusted to minimize $\log D(x|y)$ (Mirza and Osindero, 2014).

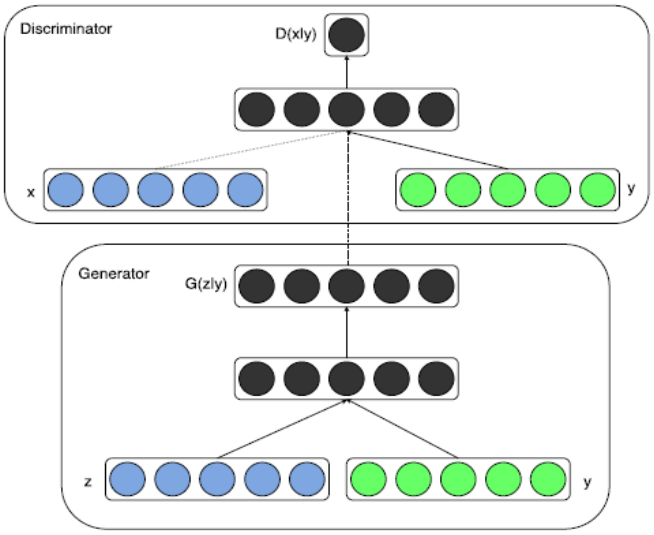

Figure 3.5: Illustration of a simple CGAN

CGAN takes advantage of the auxiliary information during the training process. The generator is fed with the labels and noise as input; it generates data that is similar to training data. The discriminator is fed with the data from the training set and the data generated from the generator. It attempts to differentiate the "real" data from "generated" data.

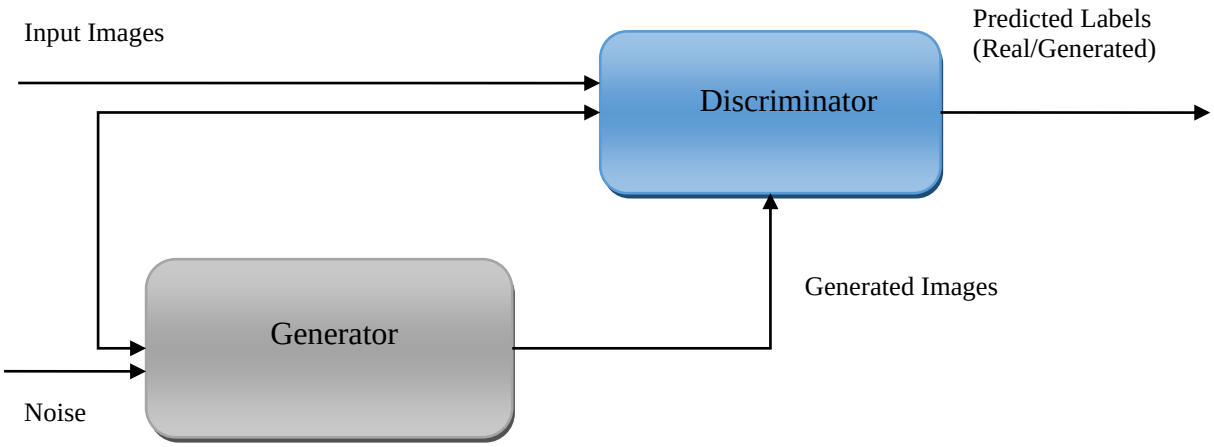

Figure 3.6: Simple representation of Conditional Generative Adversarial Network

The generator should be trained to generate data that is close to real data to confuse the discriminator. Discriminator should be trained to classify real and generated data(Train Conditional Generative Adversarial Network (CGAN) - MATLAB & Simulink, 2020).

3.4.2 U-Net

Olaf Ronneberger et al. (Ronneberger et al., 2015) proposed a network and strategy for training that is based on data augmentation for efficient use of available annotated data. The FCNs were modified and extended (Long et al., n.d.) in such a way that it can be trained with very few images but can result in more accurate segmentation. The architecture proposed in this paper consists of a contracting and an expanding path. The pooling operators are replaces with upsampling operators to increase the resolution of the output. Upsampling results in more number of feature channels, allowing the network to pass on the context information to higher resolution layers. The expansive path is almost symmetrical to the contracting path, and results in a u-shaped architecture. Contracting path resembles a CNN and captures the context. The expanding path is used for precise localization. They showed that model can perform better compared to the prior models when trained end-to-end even from a very few samples. It has repeated two convolutions of 3x3, each followed by a ReLU and a 2x2 max pooling layer for down-sampling. The number of features channels is doubled at each step of down-sampling. At each step in the expansive path, the feature map is up-sampled, followed by a convolution of 2x2 to reduce the number of features channels to half. It is concatenated with the feature map that is cropped from the contracting path, and two 3x3 convolutions, each followed by a ReLU. In the last layer, a convolution of 1x1 is used to map each 64-

component feature vector to the required number of classes. There are a total of 23 convolutional layers in the network. The model was applied for the segmentation of neuronal structures in electron microscopic recordings (EM segmentation challenge), and cell segmentation task in light microscopic images (ISBI cell tracking challenge). The u-net architecture has shown extraordinary performance on different biomedical segmentation tasks.

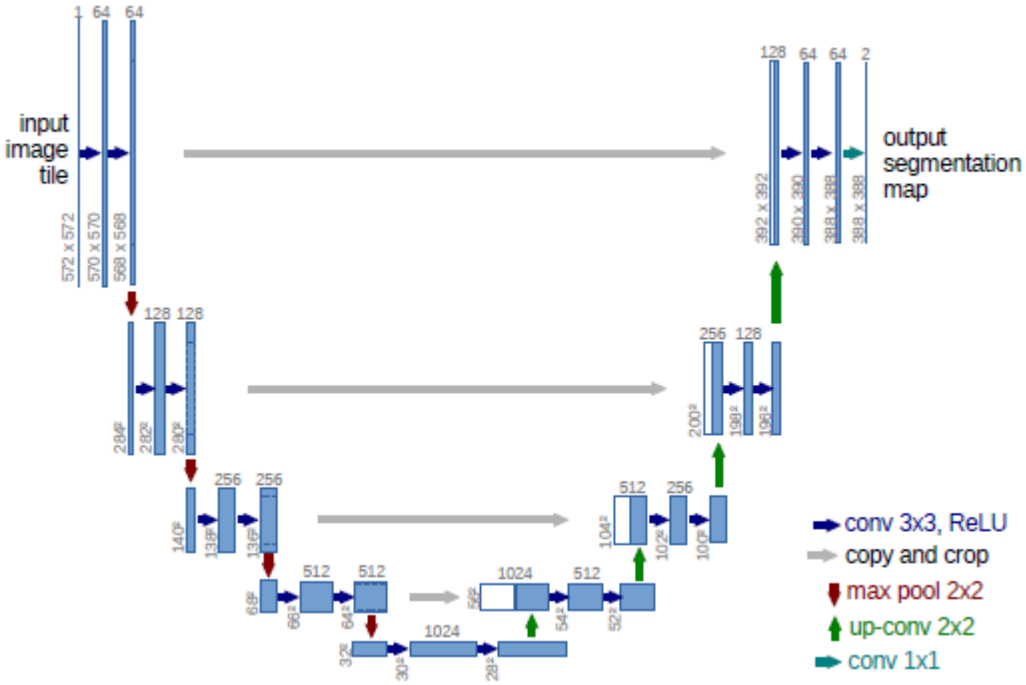

Figure 3.7: Example of U-net architecture

3.4.3 The cascaded U-Net

In 2019, Zeyu Jiang et al. (Jiang et al., 2020a)used a cascaded U-Net with two stages. The cascaded network with two stages is trained from end-to-end. A different form of U-Net is used in the first stage for coarse prediction. The raw input images and the coarse segmentation of the images from the first stage are fed to the U-Net in the second stage to get segmentation with more accuracy. To standardize MRI intensity values intensity normalization was applied to each MRI modality from each patient independently. To prevent overfitting three types of data augmentation techniques random intensity shift along with random intensity scaling, random cropping and random flipping were deployed. To overcome GPU memory limitations, the architecture was designed to take input patches of size 128x128x128 voxels with batch size one. The figures below depicts the two-stage cascaded network used by Zeyu Jiang et al. in BraTS 2019.

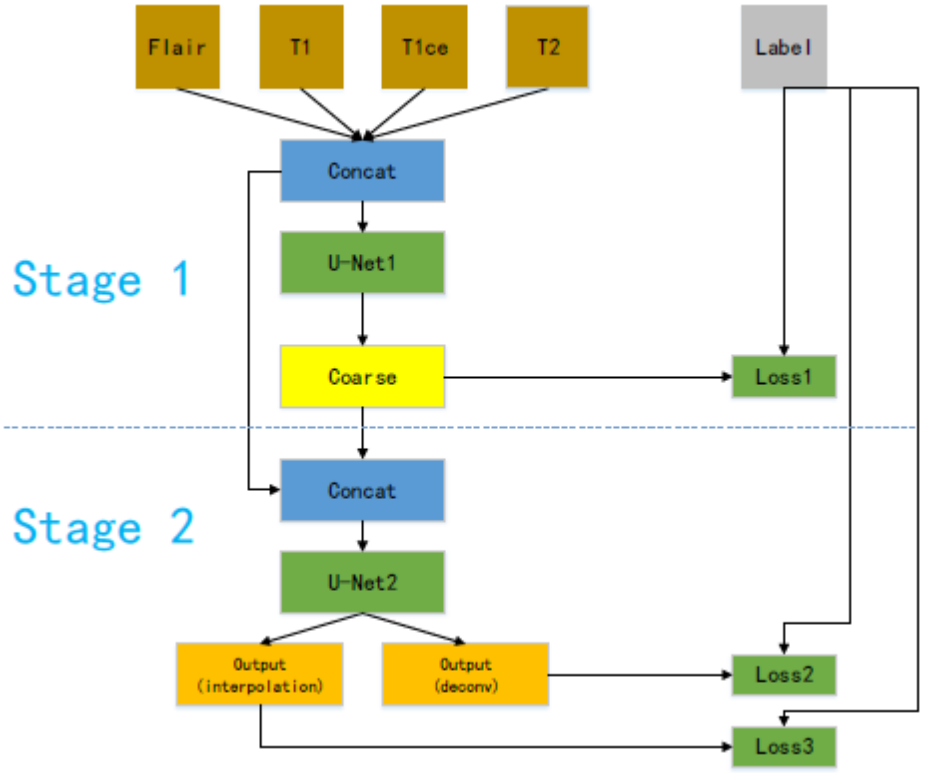

Figure 3.8: The two-stage cascaded network used by Zeyu Jiang et al. in BraTS 2019 (Jiang et al., 2020a)

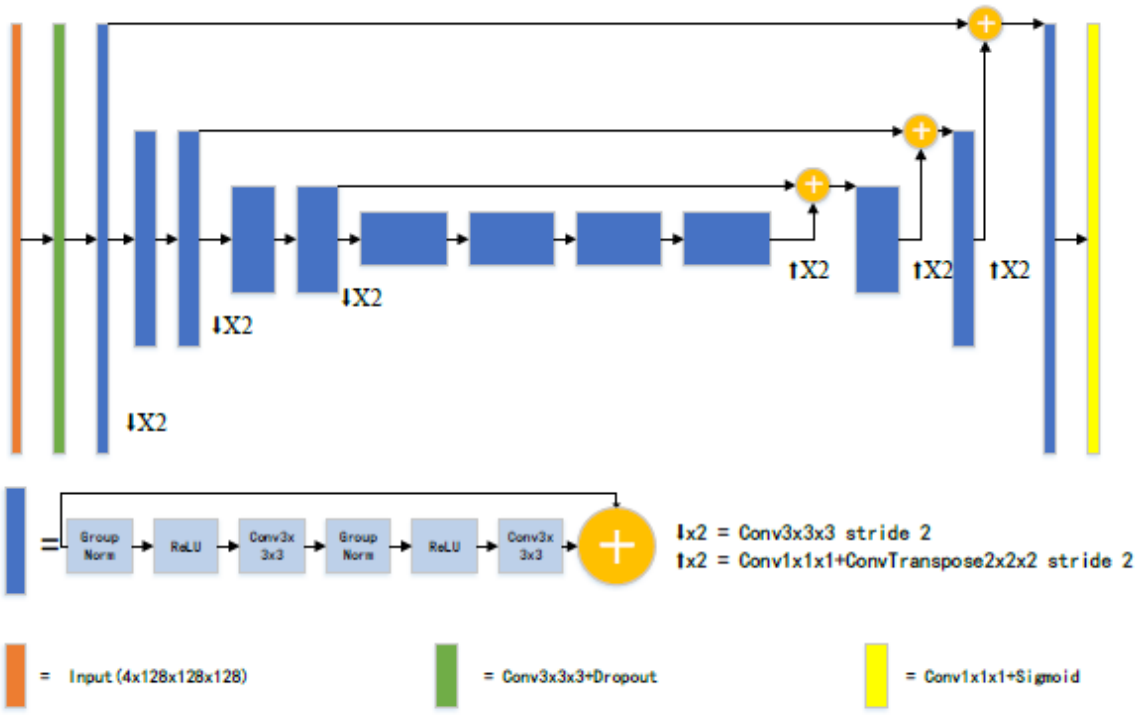

Figure 3.9: The first stage network architecture (Jiang et al., 2020a)

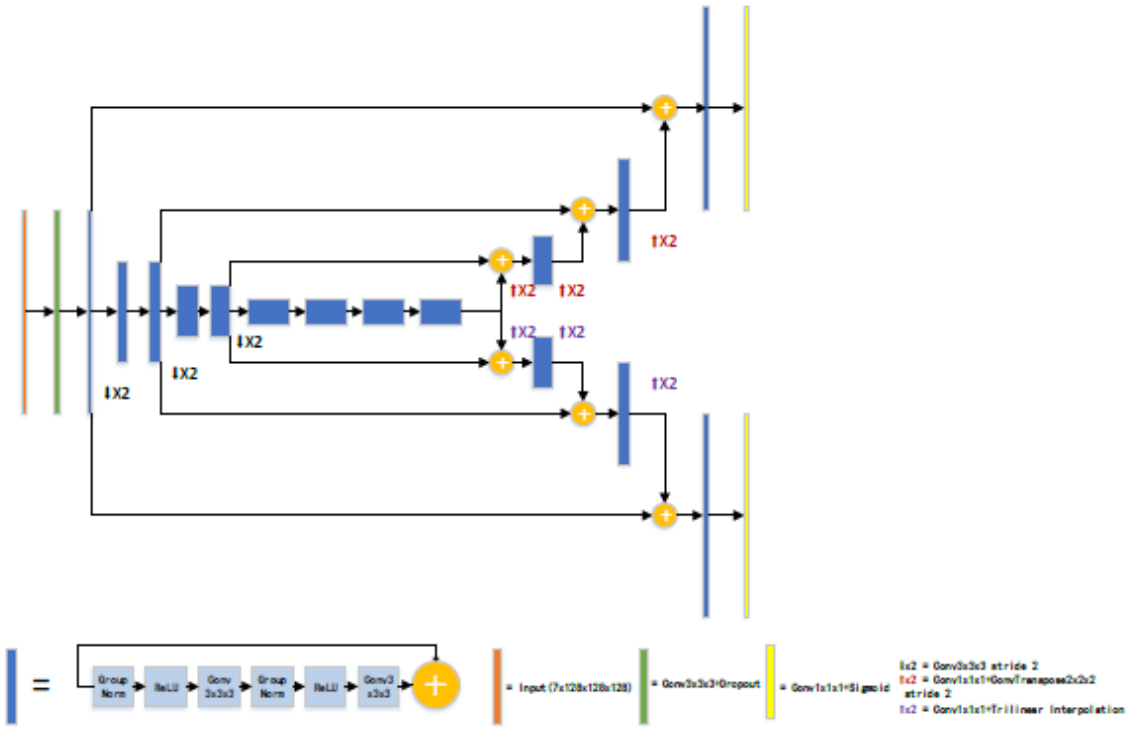

Figure 3.10: The second stage network architecture (Jiang et al., 2020a)

3.5 Summary

This chapter explains the research process followed in this research, followed by the approach used in the research. The research approach discusses the details of the dataset and its selection. As the data is in NifTI format it needs to be transformed into a format needed for the segmentation task. The images need to be pre-processed to normalize it before feeding it into the network. As a step towards well training the data, it needs to be augmented to increase the amount of data by slightly modifying the existing data. The data should be fed to the CGAN with cascaded U-Net as the generator network. The model needs to be evaluated using the segmented images based on Dice score, Hausdorff distance, sensitivity and specificity as the evaluation metrics

REFERENCES

Anon (2020) *Brain Cancer | CancerQuest*. [online] Available at: https://www.cancerquest.org/patients/cancer-type/brain-cancer?gclid=CjwKCAjwiaX8BRBZEiwAQQxGxxIbRKTcrLFRKwaLawavZh1Ekw5Lm7s5f3-525Geolli97UZnSO2RhoCUzcQAvD_BwE#footnote17_1c1lepa [Accessed 9 Nov. 2020].

Anon (2020) *Multi-modal brain tumour segmentation using deep convolutional neural networks*. [online] Available at: https://www.researchgate.net/publication/306204701_Multi-modal_brain_tumour_segmentation_using_deep_convolutional_neural_networks [Accessed 24 Nov. 2020].

Anon (2020) *Train Conditional Generative Adversarial Network (CGAN) - MATLAB & Simulink*. [online] Available at: https://www.mathworks.com/help/deeplearning/ug/train-conditional-generative-adversarial-network.html [Accessed 22 Sep. 2020].

Anon (n.d.) *NCI-MICCAI Challenge on Multimodal Brain Tumour Segmentation Proceedings of NCI-MICCAI BraTS 2013 September 22 nd , Nagoya, Japan*.

Arevalo, O., Esquenazi, Y. and Rao, M., (n.d.) The 2016 World Health Organization Classification of Tumours of the Central Nervous System: A Practical Approach for Gliomas, Part 1. Basic Tumour Genetics Spine Project View project CNS infections View project. [online] Available at: http://dx.doi.org/10.3174/ng.9170230 [Accessed 9 Nov. 2020].

Bakas, Spyridon; Akbari, Hamed; Sotiras, Aristeidis; Bilello, Michel; Rozycki, Martin; Kirby, Justin; Freymann, John; Farahani, Keyvan; Davatzikos, C., (2017) Segmentation Labels and Radiomic Features for the Pre-operative Scans of the TCGA-LGG collection. *Nat Sci Data*. [online] Available at: https://wiki.cancerimagingarchive.net/display/DOI/Segmentation+Labels+and+Radiomic+Features+for+the+Pre-operative+Scans+of+the+TCGA-LGG+collection#24282668197861a846e445a795694ff2a50eb66c.

Bakas, S., Akbari, H., Sotiras, A., Bilello, M., Rozycki, M., Kirby, J., Freymann, J., Farahani, K. and Davatzikos, C., (2017a) Segmentation labels and radiomic features for the pre-operative scans of the TCGA-GBM collection. The Cancer Imaging Archive. *Nat Sci Data*, 4, p.170117.

Bakas, S., Akbari, H., Sotiras, A., Bilello, M., Rozycki, M., Kirby, J.S., Freymann, J.B., Farahani, K. and Davatzikos, C., (2017b) Advancing The Cancer Genome Atlas glioma MRI collections with expert segmentation labels and radiomic features. *Scientific Data*, 4.

Bakas, S., Reyes, M., Jakab, A., Bauer, S., Rempfler, M., Crimi, A., Takeshi Shinohara, R., Berger, C., Min Ha, S., Rozycki, M., Prastawa, M., Alberts, E., Lipkova, J., Freymann, J.,

Kirby, J., Bilello, M., Fathallah-Shaykh, H.M., Wiest, R., Kirschke, J., Wiestler, B., Colen, R., Kwon, D., Acharya, G., Agarwal, M., Alam, M., Albiol, A., Albiol, A., Albiol, F.J., Alex, V., Allinson, N., A Amorim, P.H., Amrutkar, A., Anand, G., Andermatt, S., Arbel, T., Arbelaez, P., Avery, A., Azmat, M., Bai, W., Banerjee, S., Barth, B., Batchelder, T., Batmanghelich, K., Battistella, E., Beers, A., Belyaev, M., Bendszus, M., Benson, E., Bernal, J., Nagaraja Bharath, H., Biros, G., Bisdas, S., Brown, J., Cabezas, M., Cao, S., Cardoso, J.M., Carver, E.N., Casamitjana, A., Silvana Castillo, L., Cat, M., Cattin, P., Chagas, V.S., Chandra, S., Chang, Y.-J., Chang, S., Chang, K., Chazalon, J., Chen, S., Chen, W., Chen, J.W., Chen, Z., Cheng, K., Roy Choudhury, A., Chylla, R., Clrigues, A., Colleman, S., German Rodriguez Colmeiro, R., Combalia, M., Costa, A., Cui, X., Dai, Z., Dai, L., Alexandra Daza, L., Deutsch, E., Ding, C., Dong, C., Dong, S., Dudzik, W., Eaton-Rosen, Z., Egan, G., Escudero, G., Estienne, T., Everson, R., Fabrizio, J., Fan, Y., Himthani, N., Hsu, W., Hsu, C., Hu, X., Hu, X., Hu, Y., Hu, Y., Hua, R., Huang, T.-Y., Huang, W., Van Huffel, S., Huo, Q., Iftekharuddin, K.M., Isensee, F., Islam, M., Jackson, A.S., Jambawalikar, S.R., Jesson, A., Jian, W., Jin, P., Jeya Maria Jose, V., Jungo, A., Kainz, B., Kamnitsas, K., Kao, P.-Y., Karnawat, A., Kellermeier, T., Kermi, A., Keutzer, K., Tarek Khadir, M., Khened, M., Kickingereder, P., Kim, G., King, N., Knapp, H., Knecht, U., Kohli, L., Kong, D., Kong, X., Koppers, S., Kori, A., Krishnamurthi, G., Krivov, E., Kumar, P., Kushibar, K., Lachinov, D., Lambrou, T., Lee, J., Lee, C., Lee, Y., Chung Hai Lee, M., Lefkovits, S., Lefkovits, L., Levitt, J., Li, T., Li, H., Li, W., Li, H., Li, X., Li, Y., Li, H., Li, Z., Li, X., Li, Z., Li, X., Lin, Z.-S., Lin, F., Lio, P., Liu, C., Liu, B., Liu, X., Liu, M., Liu, J., Liu, L. and LladóLlad, X., (2019) *Identifying the Best Machine Learning Algorithms for Brain Tumour Segmentation, Progression Assessment, and Overall Survival Prediction in the BraTS Challenge*. *Sandra Gonzlez-Vill*, .

Bauer, S., Fejes, T., Slotboom, J., Wiest, R., Nolte, L.-P. and Reyes, M., (2012) Segmentation of Brain Tumour Images Based on Integrated Hierarchical Classification and Regularization. In: *MICCAI BraTS Workshop*.

Chandra, S., Vakalopoulou, M., Fidon, L., Battistella, E., Estienne, T., Sun, R., Robert, C., Deutsch, E. and Paragios, N., (2019) Context aware 3D cnns for brain tumour segmentation. In: *Lecture Notes in Computer Science (including subseries Lecture Notes in Artificial Intelligence and Lecture Notes in Bioinformatics)*.

Chen, W., Liu, B., Peng, S., Sun, J. and Qiao, X., (2019) S3D-UNET: Separable 3D U-Net for brain tumour segmentation. In: *Lecture Notes in Computer Science (including subseries Lecture Notes in Artificial Intelligence and Lecture Notes in Bioinformatics)*.

Chiu, B., (2005) Evaluation of Segmentation algorithms for Medical Imaging. *IEEE Engineering in Medicine and Biology Society*. [online] Available at: https://www.researchgate.net/publication/6522672 [Accessed 25 Nov. 2020].

Cires¸ancires¸an, D.C., Giusti, A., Gambardella, L.M. and Urgen Schmidhuber, J.¨, (n.d.) *Deep Neural Networks Segment Neuronal Membranes in Electron Microscopy Images*. [online] Available at: http://www.idsia.ch/ [Accessed 25 Nov. 2020].

Cui, S., Mao, L., Jiang, J., Liu, C. and Xiong, S., (2018) Automatic semantic segmentation of brain gliomas from MRI images using a deep cascaded neural network. *Journal of Healthcare Engineering*, 2018.

Dice, L.R., (n.d.) *MEASURES OF THE AMOUNT OF ECOLOGIC ASSOCIATION BETWEEN SPECIES*.

Dong, H., Yang, G., Liu, F., Mo, Y. and Guo, Y., (2011) *Automatic Brain Tumour Detection and Segmentation Using U-Net Based Fully Convolutional Networks*.

Dvořák, P. and Menze, B., (2016) Local structure prediction with convolutional neural networks for multimodal brain tumour segmentation. *Lecture Notes in Computer Science (including subseries Lecture Notes in Artificial Intelligence and Lecture Notes in Bioinformatics)*, 9601 LNCSOctober 2015, pp.59–71.

Ghaffari, M., Sowmya, A. and Oliver, R., (2020) Automated Brain Tumour Segmentation Using Multimodal Brain Scans: A Survey Based on Models Submitted to the BraTS 2012-2018 Challenges. *IEEE Reviews in Biomedical Engineering*, 13, pp.156–168.

Havaei, M., Davy, A., Warde-Farley, D., Biard, A., Courville, A., Bengio, Y., Pal, C., Jodoin, P.-M. and Larochelle, H., (n.d.) *Brain Tumour Segmentation with Deep Neural Networks $*.

Havaei, M., Dutil, F., Pal, C., Larochelle, H. and Jodoin, P.M., (2016) A convolutional neural network approach to brain tumour segmentation. In: *Lecture Notes in Computer Science (including subseries Lecture Notes in Artificial Intelligence and Lecture Notes in Bioinformatics)*. [online] Springer Verlag, pp.195–208. Available at: https://link.springer.com/chapter/10.1007/978-3-319-30858-6_17 [Accessed 24 Nov. 2020].

Isensee, F., Kickingereder, P., Wick, W., Bendszus, M. and Maier-Hein, K.H., (2018a) Brain tumour segmentation and radiomics survival prediction: Contribution to the BraTS 2017 challenge. In: *Lecture Notes in Computer Science (including subseries Lecture Notes in Artificial Intelligence and Lecture Notes in Bioinformatics)*.

Isensee, F., Kickingereder, P., Wick, W., Bendszus, M. and Maier-Hein, K.H., (n.d.) *No New-Net*.

Isensee, F., Petersen, J., Klein, A., Zimmerer, D., Jaeger, P.F., Kohl, S., Wasserthal, J.,

Köhler, G., Norajitra, T., Wirkert, S. and Maier-Hein, K.H., (2018b) *nnU-Net: Self-adapting framework for u-net-based medical image segmentation*. *arXiv*.

Jiang, Z., Ding, C., Liu, M. and Tao, D., (2020a) Two-stage cascaded u-net: 1st place solution to brats challenge 2019 segmentation task. In: *Lecture Notes in Computer Science (including subseries Lecture Notes in Artificial Intelligence and Lecture Notes in Bioinformatics)*. Springer, pp.231–241.

Jiang, Z., Ding, C., Liu, M. and Tao, D., (2020b) Two-stage cascaded u-net: 1st place solution to brats challenge 2019 segmentation task. *Lecture Notes in Computer Science (including subseries Lecture Notes in Artificial Intelligence and Lecture Notes in Bioinformatics)*, 11992 LNCSAugust, pp.231–241.

Kamnitsas, K., Bai, W., Ferrante, E., Mcdonagh, S., Sinclair, M., Pawlowski, N., Rajchl, M., Lee, M., Kainz, B., Rueckert, D. and Glocker, B., (n.d.) *Ensembles of Multiple Models and Architectures for Robust Brain Tumour Segmentation*.

Kamnitsas, K., Ferrante, E., Parisot, S., Ledig, C., Nori, A., Criminisi, A., Rueckert, D. and Glocker, B., (n.d.) *DeepMedic for Brain Tumour Segmentation*. [online] Available at: https://github.com/Kamnitsask/deepmedic [Accessed 24 Nov. 2020b].

Kamnitsas, K., Ledig, C., Newcombe, V.F.J., Simpson, J.P., Kane, A.D., Menon, D.K., Rueckert, D. and Glocker, B., (2017) Efficient multi-scale 3D CNN with fully connected CRF for accurate brain lesion segmentation. *Medical Image Analysis*, 36, pp.61–78.

Krizhevsky, A., Sutskever, I. and Hinton, G.E., (2017) ImageNet Classification with Deep Convolutional Neural Networks. *COMMUNICATIONS OF THE ACM*, [online] 606. Available at: http://code.google.com/p/cuda-convnet/. [Accessed 24 Nov. 2020].

Lachinov, D., Vasiliev, E. and Turlapov, V., (2019) Glioma segmentation with cascaded UNet. *Lecture Notes in Computer Science (including subseries Lecture Notes in Artificial Intelligence and Lecture Notes in Bioinformatics)*, 11384 LNCS, pp.189–198.

Larobina, M. and Murino, L., (n.d.) Medical Image File Formats.

Li, C. and Wand, M., (n.d.) *Precomputed Real-Time Texture Synthesis with Markovian Generative Adversarial Networks*. [online] Available at: https://github.com/chuanli11/MGANs [Accessed 11 Nov. 2020].

Liu, J., Li, M., Wang, J., Wu, F., Liu, T. and Pan, Y., (2014) *A survey of MRI-based brain tumour segmentation methods*. *Tsinghua Science and Technology*, .

Long, J., Shelhamer, E. and Darrell, T., (n.d.) *Fully Convolutional Networks for Semantic Segmentation*.

Louis, D.N., Perry, A., Reifenberger, G., von Deimling, A., Figarella-Branger, D., Cavenee,

W.K., Ohgaki, H., Wiestler, O.D., Kleihues, P. and Ellison, D.W., (2016) *The 2016 World Health Organization Classification of Tumours of the Central Nervous System: a summary*. *Acta Neuropathologica*, .

Luc, P., Couprie, C., Chintala, S. and Verbeek, J., (n.d.) *Semantic Segmentation using Adversarial Networks*.

Maas, A.L., Hannun, A.Y. and Ng, A.Y., (2013) *Rectifier Nonlinearities Improve Neural Network Acoustic Models*.

Menze, B., Reyes, M., Jakab, A., Gerstner, E., Kirby, J. and Farahani, K., (2013) *Proceedings of the MICCAI Challenge on Multimodal Brain Tumour Image Segmentation (BraTS) 2013*. [online] Japan. MICCAI. Available at: https://hal.inria.fr/hal-00912934 [Accessed 24 Nov. 2020].

Menze, B.H., Jakab, A., Bauer, S., Kalpathy-Cramer, J., Farahani, K., Kirby, J., Burren, Y., Porz, N., Slotboom, J., Wiest, R., Lanczi, L., Gerstner, E., Weber, M.A., Arbel, T., Avants, B.B., Ayache, N., Buendia, P., Collins, D.L., Cordier, N., Corso, J.J., Criminisi, A., Das, T., Delingette, H., Demiralp, Ç., Durst, C.R., Dojat, M., Doyle, S., Festa, J., Forbes, F., Geremia, E., Glocker, B., Golland, P., Guo, X., Hamamci, A., Iftekharuddin, K.M., Jena, R., John, N.M., Konukoglu, E., Lashkari, D., Mariz, J.A., Meier, R., Pereira, S., Precup, D., Price, S.J., Raviv, T.R., Reza, S.M.S., Ryan, M., Sarikaya, D., Schwartz, L., Shin, H.C., Shotton, J., Silva, C.A., Sousa, N., Subbanna, N.K., Szekely, G., Taylor, T.J., Thomas, O.M., Tustison, N.J., Unal, G., Vasseur, F., Wintermark, M., Ye, D.H., Zhao, L., Zhao, B., Zikic, D., Prastawa, M., Reyes, M. and Van Leemput, K., (2015) The Multimodal Brain Tumour Image Segmentation Benchmark (BraTS). *IEEE Transactions on Medical Imaging*, 3410, pp.1993–2024.

Milletari, F., Navab, N. and Ahmadi, S.A., (2016) V-Net: Fully convolutional neural networks for volumetric medical image segmentation. *Proceedings - 2016 4th International Conference on 3D Vision, 3DV 2016*, pp.565–571.

Mirza, M. and Osindero, S., (2014) Conditional Generative Adversarial Nets. [online] Available at: http://arxiv.org/abs/1411.1784.

Myronenko, A., (2019) 3D MRI brain tumour segmentation using autoencoder regularization. In: *Lecture Notes in Computer Science (including subseries Lecture Notes in Artificial Intelligence and Lecture Notes in Bioinformatics)*. pp.311–320.

Openai, I.G., (n.d.) *NIPS 2016 Tutorial: Generative Adversarial Networks*. [online] Available at: http://www.iangoodfellow.com/slides/2016-12-04-NIPS.pdf [Accessed 12 Nov. 2020].

Pereira, S., Pinto, A., Alves, V. and Silva, C.A., (2016) Brain Tumour Segmentation Using

Convolutional Neural Networks in MRI Images. *IEEE TRANSACTIONS ON MEDICAL IMAGING*, [online] 355. Available at: http://www.ieee.org/publications_standards/publications/rights/index.html [Accessed 10 Nov. 2020].

Randhawa, R.S., Modi, A., Jain, P. and Warier, P., (n.d.) Improving Boundary Classification for Brain Tumour Segmentation and Longitudinal Disease Progression.

Rezaei, M., Harmuth, K., Gierke, W., Kellermeier, T., Fischer, M., Yang, H. and Meinel, C., (n.d.) *Conditional Adversarial Network for Semantic Segmentation of Brain Tumour*.

Ronneberger, O., Fischer, P. and Brox, T., (2015) U-net: Convolutional networks for biomedical image segmentation. In: *Lecture Notes in Computer Science (including subseries Lecture Notes in Artificial Intelligence and Lecture Notes in Bioinformatics)*. pp.234–241.

Simonyan, K. and Zisserman, A., (2015) *VERY DEEP CONVOLUTIONAL NETWORKS FOR LARGE-SCALE IMAGE RECOGNITION*. [online] Available at: http://www.robots.ox.ac.uk/ [Accessed 24 Nov. 2020].

Singh, V.K., Romani, S., Rashwan, H.A., Akram, F., Pandey, N., Sarker, M.M.K., Abdulwahab, S., Torrents-Barrena, J., Saleh, A., Arquez, M., Arenas, M. and Puig, D., (2018) Conditional generative adversarial and convolutional networks for X-ray breast mass segmentation and shape classification. In: *Lecture Notes in Computer Science (including subseries Lecture Notes in Artificial Intelligence and Lecture Notes in Bioinformatics)*. pp.833–840.

Szegedy, C., Liu, W., Jia, Y., Sermanet, P., Reed, S., Anguelov, D., Erhan, D., Vanhoucke, V. and Rabinovich, A., (n.d.) *Going Deeper with Convolutions*.

Taha, A.A. and Hanbury, A., (2015a) An Efficient Algorithm for Calculating the Exact Hausdorff Distance. *IEEE Transactions on Pattern Analysis and Machine Intelligence*, 3711, pp.2153–2163.

Taha, A.A. and Hanbury, A., (2015b) Metrics for evaluating 3D medical image segmentation: Analysis, selection, and tool. *BMC Medical Imaging*, [online] 151, pp.1–28. Available at: https://link.springer.com/articles/10.1186/s12880-015-0068-x [Accessed 9 Nov. 2020].

Wang, G., Li, W., Ourselin, S. and Vercauteren, T., (n.d.) *Automatic Brain Tumour Segmentation using Cascaded Anisotropic Convolutional Neural Networks*.

Wen, P.Y. and Kesari, S., (2008) *Medical Progress Malignant Gliomas in Adults*. [online] *N Engl J Med*, Available at: www.nejm.org [Accessed 9 Nov. 2020].

Wu, Y. and He, K., (n.d.) *Group Normalization*.

Zhao, X., Wu, Y., Song, G., Li, Z., Zhang, Y. and Fan, Y., (2018) A deep learning model

integrating FCNNs and CRFs for brain tumour segmentation. *Medical Image Analysis*, 43.

Zhao, Y.X., Zhang, Y.M. and Liu, C.L., (2020) Bag of tricks for 3d mri brain tumour segmentation. In: *Lecture Notes in Computer Science (including subseries Lecture Notes in Artificial Intelligence and Lecture Notes in Bioinformatics)*. [online] Springer, pp.210–220. Available at: https://link.springer.com/chapter/10.1007/978-3-030-46640-4_20 [Accessed 24 Nov. 2020].

Zhou, C., Ding, C., Wang, X., Lu, Z. and Tao, D., (2020) One-Pass Multi-Task Networks with Cross-Task Guided Attention for Brain Tumour Segmentation. *IEEE Transactions on Image Processing*, 29July, pp.4516–4529.

Zikic, D., Glocker, B., Konukoglu, E. and Shotton, J., (2012) Context-Sensitive Classification Forests for Segmentation of Brain Tumour Tissues. *Proc MICCAI-BraTS (Multimodal Brain Tumour Segmentation Challenge)*.

Zikic, D., Ioannou, Y., Brown, M. and Criminisi, A., (n.d.) *Segmentation of Brain Tumour Tissues with Convolutional Neural Networks*.

Zou, K.H., Warfield, S.K., Bharatha, A., Tempany, C.M.C., Kaus, M.R., Haker, S.J., Wells, W.M., Jolesz, F.A. and Kikinis, R., (2004) Statistical Validation of Image Segmentation Quality Based on a Spatial Overlap Index. *Academic Radiology*, [online] 112, pp.178–189. Available at: /pmc/articles/PMC1415224/?report=abstract [Accessed 25 Nov. 2020].

APPENDIX A: RESEARCH PLAN

The below figure shows the plan for this research represented as a Gantt chart.

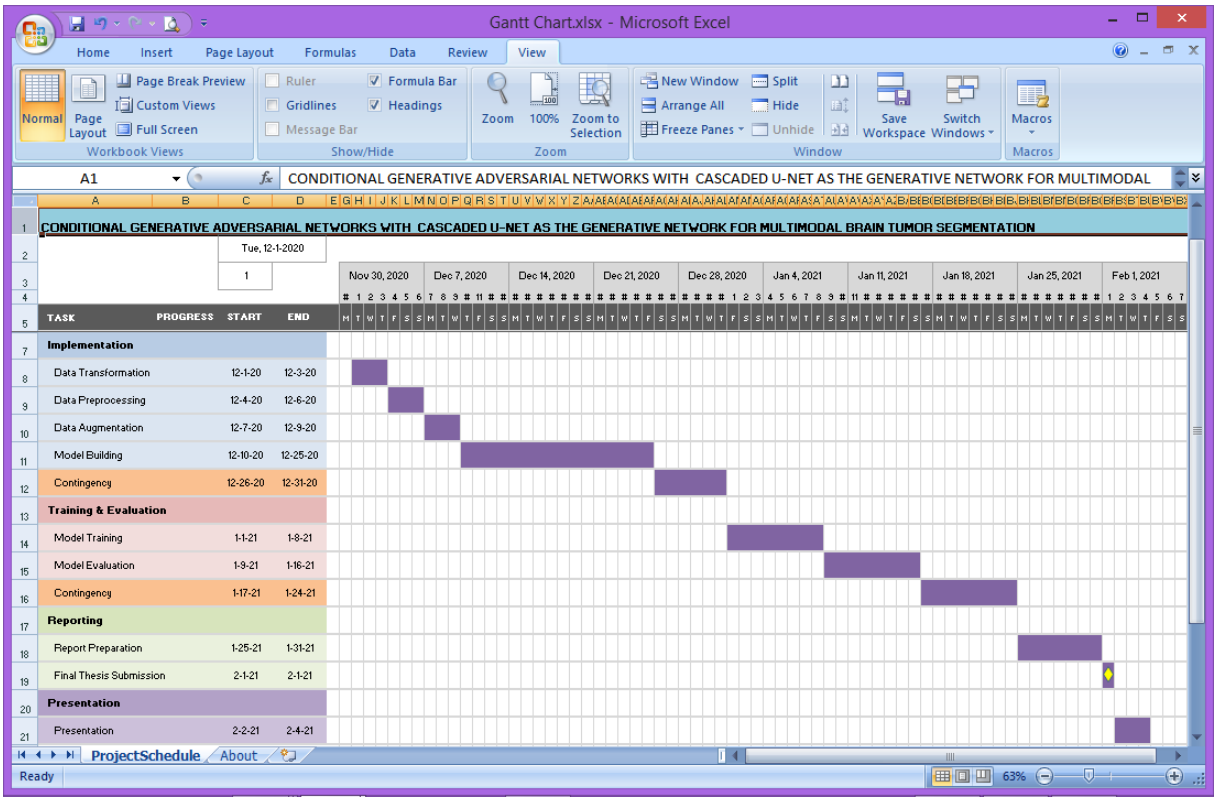

APPENDIX B: RESEARCH PROPOSAL

CONDITIONAL GENERATIVE ADVERSARIAL NETWORKS
FOR
MULTIMODAL BRAIN TUMOR SEGMENTATION

SUSHMA PODISHETTI
(Student Id: 931050)
M.Sc. in Data Science,
Liverpool John Moore's University
Supervisor: Shah Ayub Quadri

Research Proposal

SEPTEMBER 2020

Abstract

The most commonly occurring tumors in the brain that originate from glial cells and infiltrate the tissues surrounding them are gliomas. Gliomas are inherently heterogeneous concerning their histology, shape, and appearance. Because of their heterogeneous nature, it is very challenging to segment gliomas sub-regions in Magnetic Resonance Imaging (MRI) scans. Replacing the traditional procedures with the state-of-the-art methods for segmentation of glioma sub-regions in the MRI scans would be of great value for better diagnosis, treatment planning, and follow-up. It would also save doctors time. This paper proposes a state-of-the-art neural network architecture that is based on the Conditional Generative Adversarial Network (CGAN) for the automatic segmentation of glioma sub-regions. The CGANs can accurately segment the tumor with its generator and discriminator network. The generative network learns the inherent heterogeneity of gliomas and challenges the adversarial network on its ability to differentiate between real and generated images. The adversarial network challenges the generative network by segmenting the tumors accurately. This results in improved accuracy of the segmentation. Experiments will be performed on multimodal MRI brain scans from the BraTS 2020 challenge. The model is expected to segment glioma sub-regions (the enhancing tumor (ET), the peritumoral edema (ED), the non-enhancing tumor core (NET), and the necrotic (NCR)). The metrics Dice score, specificity, sensitivity, and Hausdorff distance will be used to evaluate the performance of the model.

Keywords:

Brain Tumor Segmentation, Gliomas, MRI, Conditional Generative Adversarial Network,

U-Net, CGAN,Glioma sub-regions

Table of Contents

Abstract 43
1. Introduction 47
1.1 Background 47
1.2 Dataset 47
2. Related Work 50
3. Research Questions 51
4. Aim and Objectives 51
5. Significance of this study 51
6. Scope of this study 52
7. Research Methodology 52
7.1 Proposed Model 52
7.2 Conditional Generative Adversarial Networks 53
7.3 U-Net 55
7.4 Process 56
8. Requirements/Resources 56
8.1 Hardware 56
8.2 Software 57
8.3 Technical skills 57
8.4 Domain Knowledge 57
9. Research Plan 58
Reference 59

LIST OF FIGURES

Figure 1: Different image modalities of brain from BraTS dataset(Jiang et al., 2020).....48
Figure 2: Sections of brain images with gliomas sub-regions in different MRI modalities (http://braintumorsegmentation.org/) 49
Figure 3: Proposed model - CGAN with U-Net as the generative network. 53
Figure 4: Illustration of a simple CGAN. 54
Figure 5: Simple representation of Conditional Generative Adversarial Network 54
Figure 6: Example of U-net architecture 55
Figure 7 : Flow chart representing the research process 56
Figure 8 : Gantt chart showing the research plan. 58

LIST OF ABBREVIATIONS

.....Magnetic Resonance Imaging
CGAN.....Conditional Generative Adversarial Network
BraTS..... Brain Tumor Segmentation
CT.....Computed Tomography
LGG.....Low-Grade Gliomas
HGG.....High-Grade Gliomas
Gd..... Gadolinium
FLAIR.....Fluid Attenuated Inversion Recovery
CSF.....Cerebrospinal Fluid
ET.....Enhancing Tumor
ED.....Edema
NET.....Non-Enhancing Tumor Core
NCR.....Necrotic
TC.....Tumor Core
WT.....Whole Tumor
CNN.....Convolutional Neural Network
VAE.....Variational Auto Encoder
ROI..... Region of Interest
ReLU.....Rectified Linear Unit

1. Introduction

1.1 Background

This study focuses on segmentation of glioma sub-regions. These brain tumors start from the glial cells. Glial cells support the function of the neurons. They commonly occur in the cerebral hemispheres of the brain. They can also happen in the brain stem, the optic nerves, and the cerebellum. They can be benign or malignant. The exact cause of gliomas is not known. They contribute about one-third of all brain tumors.

Gliomas are diagnosed based on medical history, physical examination, neurological examination, images of the brain, and biopsy. Magnetic resonance imaging (MRI) and computed tomography (CT) scans are used most commonly to diagnose brain tumors and to check for tumor growth after the treatment.

Gliomas are classified into grades I, II, III & IV. These four grades of gliomas are grouped into "Low-Grade Gliomas (LGG)" (grade I or grade II) and "High-Grade Gliomas (HGG)" (grade III or grade IV) based on the tumor's aggressiveness and growth potential. The treatment for gliomas depends on its grade. The patients with HGG can survive for two years or less and would need treatment immediately. The patients with LGG can survive for several years, and aggressive treatment can be delayed. For both grades of gliomas, multimodal brain images are used before and after treatment to diagnose, check the tumor progression, and to evaluate the treatment strategy.

1.2 Dataset

The experiment will be performed on the brain MRI scans from BraTS 2020 challenge. The data set contains training set and validation set. The training dataset contains the MRI scans of 369 patients, and the validation dataset has MRI scans of 125 patients(Menze et al., 2015; Bakas et al., 2017b; a, 2018; Bakas, Spyridon; Akbari, Hamed; Sotiras, Aristeidis; Bilello, Michel; Rozycki, Martin; Kirby, Justin; Freymann, John; Farahani, Keyvan; Davatzikos, 2017).

The dataset provides the below types of brain images for each patient.

- Native T1 (T1) (T1 images highlight fat tissue within the body)
- Post-contrast T1-weighted (T1-Gd) (Gadolinium is the most commonly used contrast agent for MRI. Abnormal tissue may enhance more than surrounding normal tissue following intravenous gadolinium)
- T2-weighted (T2) (T2 images highlight fat and water within the body) and
- T2 Fluid Attenuated Inversion Recovery (T2-FLAIR) (The signal from a free fluid such as cerebrospinal fluid (CSF) is suppressed on the images)

The figure below (Figure 1) shows the T2 Flair, T1 weighted, T1 post-contrast, and T2 weighted image modalities of the brain.

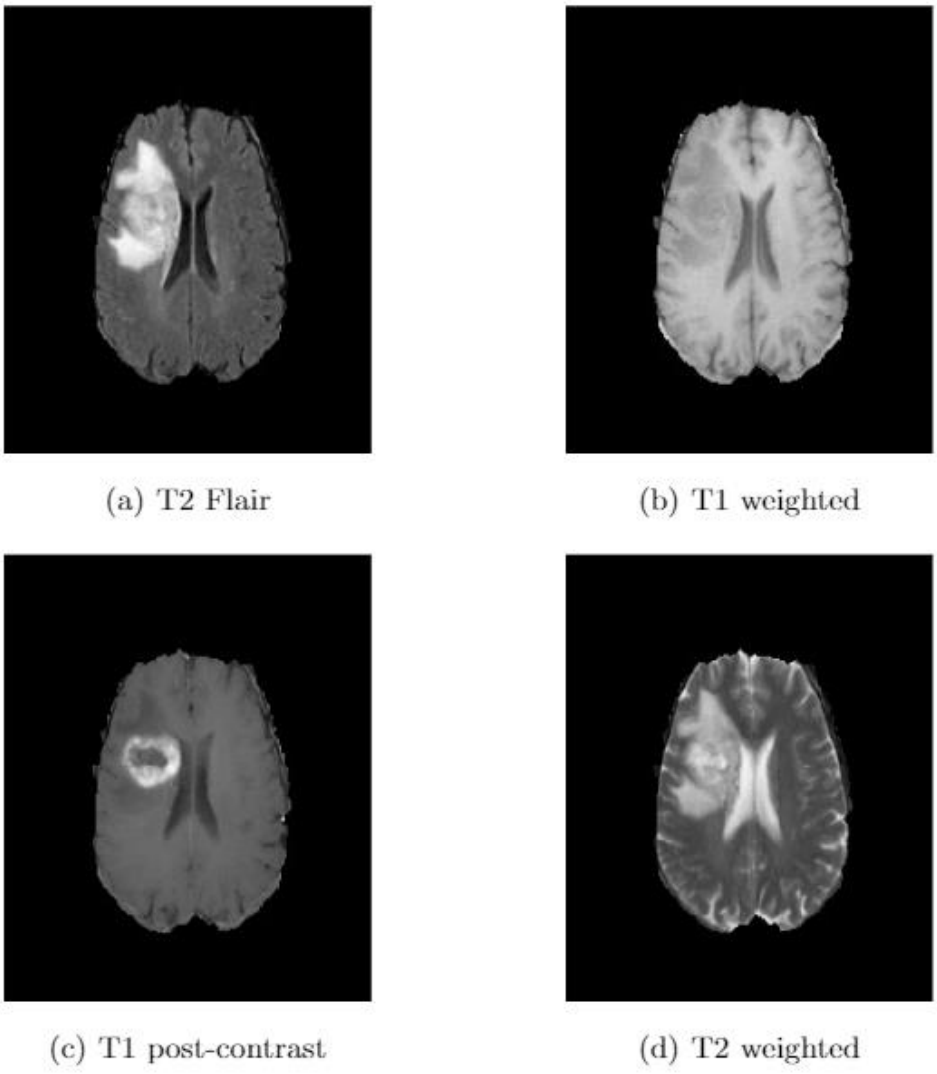

Figure 7: Different image modalities of brain from BraTS dataset(Jiang et al., 2020)

Each tumor is further segmented into the following sub-regions, the peritumoral edema, the enhancing tumor, and the necrotic and non-enhancing tumor core. All the brain images have been annotated manually into the necrotic and non-enhancing tumor core (NCR/NET - label 1), the peritumoral edema (ED - label 2) and, GD-enhancing tumor (ET- label 4).

The figure below (Figure 2) shows the sections of the brain image with glioma sub-regions in different modalities of brain MRI scans. Figure A shows the whole tumor (WT) visible in T2-FLAIR (in yellow). Figure B shows the tumor core (TC) visible in T2 (in orange). Figure C shows the enhancing tumor (ET) visible in T1-Gd (in light blue), that surrounds the cystic/necrotic components of the core (in green). Figure D shows the combination of segmentations along with the labels of glioma sub-regions

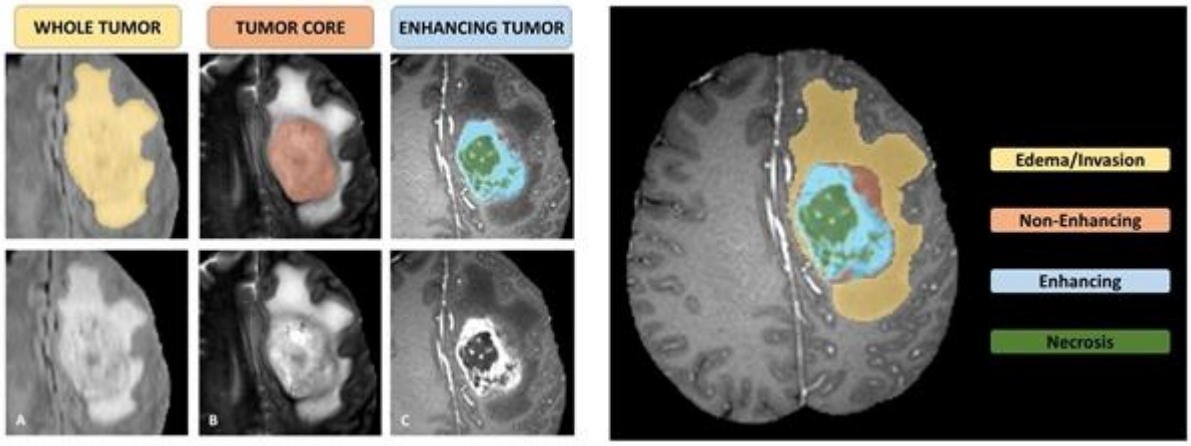

Figure 8: Sections of brain images with gliomas sub-regions in different MRI modalities (http://braintumorsegmentation.org/)

As it is time consuming, tedious, and requires a lot of attention to segment the gliomas sub-regions manually, it becomes extremely important to fully automate this process for improved diagnosis, treatment planning, follow-up and to assess the way the tumor progresses. It would also save doctors time (Lachinov et al., 2020). This paper proposes a neural network architecture based on CGAN with U-Net as generator for improved segmentation of glioma sub-regions.

2. Related Work

In the BraTS challenge 2018 Myronenko (Myronenko, 2019), used a CNN architecture based on the encoder-decoder model. The model has a larger encoder for extracting features of the image, and a smaller decoder for reconstructing the segmentation mask. The encoder part of the network uses ResNet blocks with GroupNorm normalization. The image is spatially downsized to eight times smaller than the input image at the encode endpoint. The decoder is similar in structure to the encoder. The spatial size and the number of features of the image at the decoder endpoint are the same as the original image. The segmentation decoder output has three channels followed by a sigmoid to classify the tumor sub-regions (TC, WT, and ET). A variational auto-encoder (VAE) branch is used for regularization and guidance to the encoder(Myronenko, 2019).

In the BraTS challenge 2019, Zeyu Jiang et al. (Jiang et al., 2020) used a cascaded U-Net with two stages. A different form of U-Net is used in the first stage for coarse prediction. The raw input images and the coarse segmentation of the image from the first stage are fed to the U-Net in the second stage to get segmentation with more accuracy. The first stage architecture has a larger encoding path, for extracting complex features and a smaller decoding path, for getting segmentation map with the size the same as the input image. In the second stage, the number of filters is doubled to increase the network width. It uses two decoders(Jiang et al., 2020).

In 2018, Vivek Kumar Singh et al. (Singh et al., 2018) proposed an approach for breast mass segmentation in mammography based on CGAN. The generator part of the CGAN is used in the first stage to obtain a binary mask that selects the pixels that represent the area of the breast mass and ignores the pixels that represent the healthy tissue. The mammogram cropped to contain the mass ROI. The image was regularized with a Gaussian filter for noise removal. The second stage contains a CNN to classify the binary mask obtained in the first stage into one of the 4 classes of mass shape (round, oval, lobular, and irregular)(Singh et al., 2018).

Inspired by the above works, hypothesized a neural network architecture based on CGAN with U-Net as generator for improved segmentation of glioma sub-regions in the multimodal MRI scans.

3. Research Questions

Can any improvement in the automatic segmentation of the glioma sub-regions be achieved by using state-of-the-art architectures in neural networks?

4. Aim and Objectives

The main aim of this research is to propose a model for the automatic segmentation of glioma sub-regions. The automatic segmentation of glioma sub-regions in the brain images is of great importance as it helps in easy, quick, and better diagnosis, giving required treatment in time, assessment of tumor progression before and after treatment, and also to check the success of the treatment strategy.

The research objectives formulated based on the aim of this study are as follows:

5. To analyze the multimodal MRI brain scans to understand the modalities of the scans and the various sub-regions of the tumors.
6. To analyze various state-of-the-art architectures that can be used for automatic segmentation of the glioma sub-regions.
7. To identify a most suitable architecture for automatic segmentation of glioma sub-regions
8. To evaluate the model performance based on the model evaluation metrics.

5. Significance of this study

This study helps in finding if the brain tumor, gliomas, and its sub-regions can be segmented with improved accuracy. Finding a fully automated model for accurately segmenting the brain tumors would help the neurologists and neurosurgeons for better diagnosis, in the assessment of tumor progression, in treatment planning, and follow-up. It would also save doctors time. It helps the patients to get timely and proper treatment as it is very important for the patients suffering from high-grade gliomas (HGG) to get required treatment on time.

6. Scope of this study

As part of this work, the performance of the CGAN with U-Net as generator for segmentation of glioma sub-regions will be studied. The other state-of-the-art architectures are out of the scope of this research. This research will be done on the BraTS 2020 challenge data set. It includes brain images of 369 patients as the training data set and brain images of 125 patients as the validation data set. Brain images from any other source are not included in this study.

7. Research Methodology

7.1 Proposed Model

The proposed architecture will use Conditional Generative Adversarial Networks with U-Net as the generator. The metrics Hausdorff distance, Dice score, specificity, and sensitivity will be used to evaluate the performance of the model.

The following are the reasons for selecting the above architecture for the segmentation of gliomas sub-regions:

- Gliomas are inherently heterogeneous (in shape, appearance, and histology) in nature. Due to the highly heterogeneous appearance, it is a very challenging task to segment gliomas in multimodal MRI brain scans. The generative network in CGAN learns the intrinsic heterogeneity of gliomas and challenges the adversarial network on its ability to distinguish between real and generated images. The adversarial network in CGAN challenges the generative network by segmenting the tumors accurately. This results in improved performance.
- U-Net performs very well and is the most widely used architecture in the segmentation of medical images.

The model proposed in this paper will use CGAN with U-Net as the generative network for the segmentation of gliomas sub-regions.

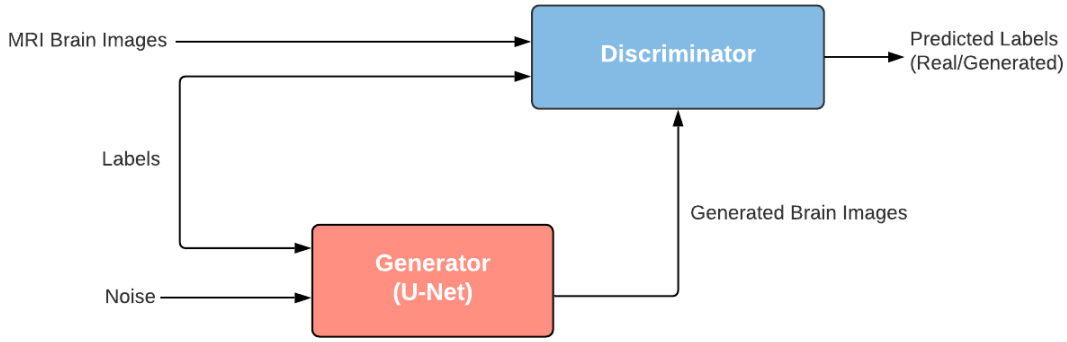

Figure 9: Proposed model - CGAN with U-Net as the generative network.

7.2 Conditional Generative Adversarial Networks

In Conditional Generative Adversarial Networks, the generator and discriminator are conditioned on some auxiliary information y, such as class labels or data from other modalities. The generator and discriminator both can be conditioned by feeding them extra information as an additional input layer.

The input noise and labels are presented as input to the generator. The discriminator is fed with real data, generated data, and labels.

CGANS use the below minmax loss function as the objective function:

$$\min_{G}\max_{D} V(D,G) = E_{x\sim pdata(x)}[\log D(x|y)] + E_{z\sim pz(z)}\left[\log\left(1 - D\left(G(z|y)\right)\right)\right]$$

In the above function, D represents discriminator, G represents generator, x represents input data, y represents labels, and z represents noise.

To train a CGAN, both the generative and discriminative networks are trained simultaneously to maximize the performance. The parameters of G(generator) are adjusted to minimize $\log\left(1 - D\left(G(z|y)\right)\right)$ and the parameters of D(discriminator) are adjusted to minimize $\log D(x|y)$ (Mirza and Osindero, 2014).

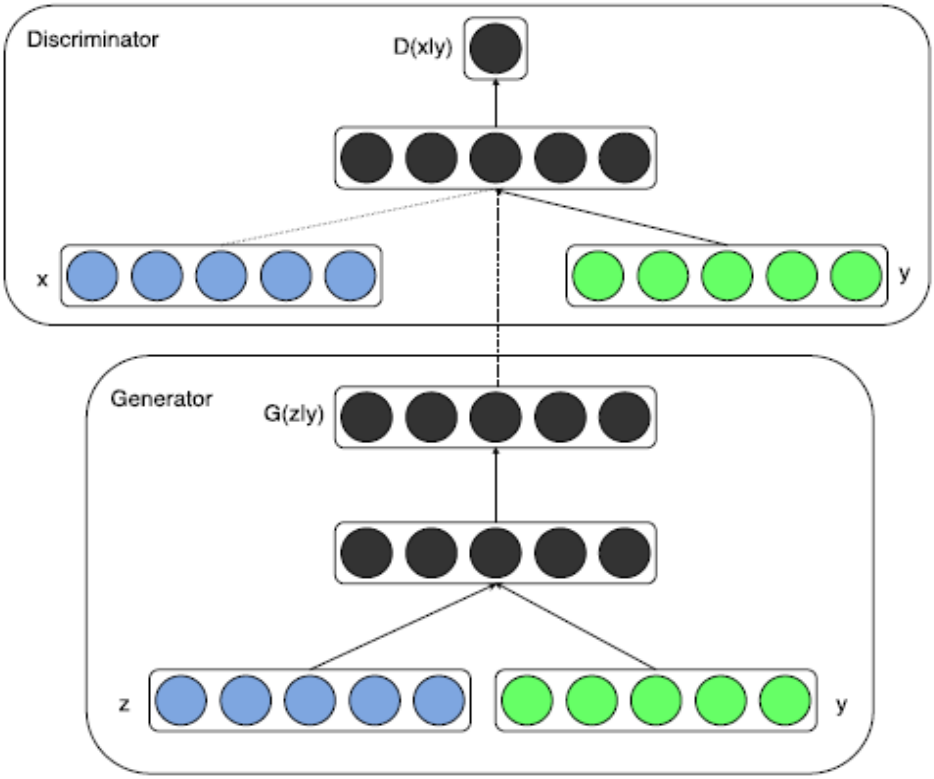

Figure 10: Illustration of a simple CGAN.

CGAN takes advantage of the auxiliary information during the training process. The generator is fed with the labels and noise as input; it generates data that is similar to training data. The discriminator is fed with the data from the training set and the data generated from the generator. It attempts to differentiate the "real" data from "generated" data.

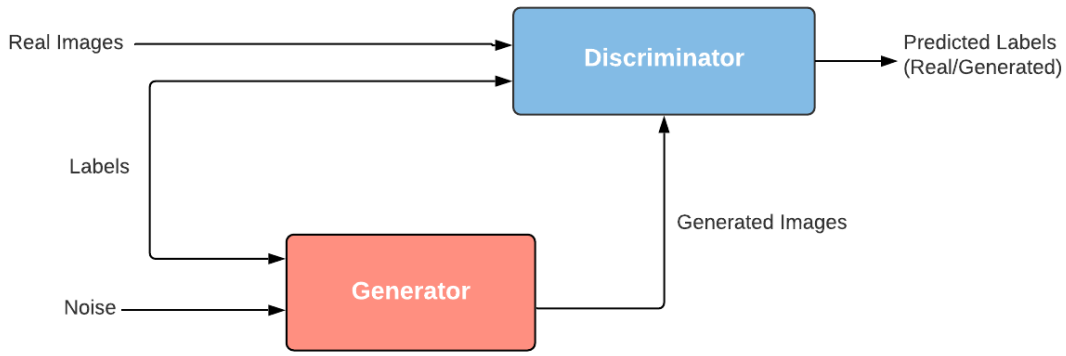

Figure 11: Simple representation of Conditional Generative Adversarial Network

The generator should be trained to generate data that is close to real data to confuse the discriminator. Discriminator should be trained to classify real and generated data(Train Conditional Generative Adversarial Network (CGAN) - MATLAB & Simulink, 2020).

7.3 U-Net

The U-Net architecture illustrated in the figure below (Figure.5) shows an example for 32x32 pixels. It has a contracting path on the left side that resembles a convolutional neural network and an expansive path on the right side. It has repeated two convolutions of 3x3, each followed by a rectified linear unit (ReLU) and a max pooling layer of 2x2 for downsampling. The number of features channels is doubled at each step of downsampling. At each step in the expansive path, the feature map is upsampled, followed by a convolution of 2x2 to reduce the number of features channels to half. It is concatenated with the cropped feature map from the contracting path, and two convolutions of 3x3, each followed by a ReLU. In the final layer, a convolution of 1x1 is used to map each 64-component feature vector to the required number of classes. There are a total of 23 convolutional layers in the network (Ronneberger et al., 2015).

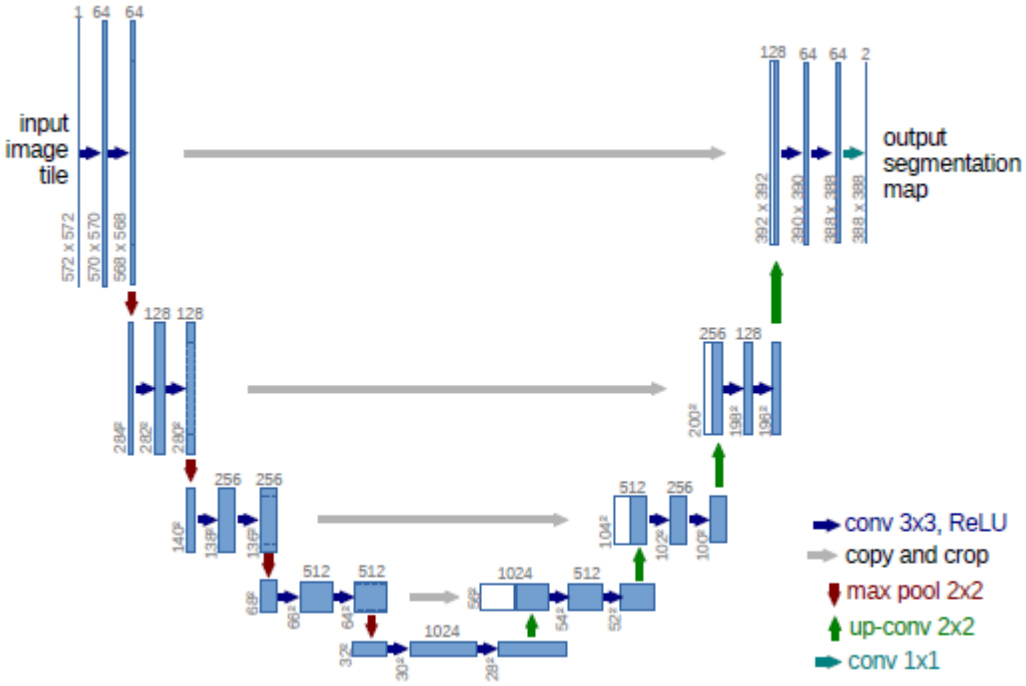

Figure 12: Example of U-net architecture

7.4 Process

The following flow chart shows the process that will be followed in this research. The performance metrics Dice score, specificity, sensitivity, and Hausdorff distance will be used to evaluate the performance of the model.

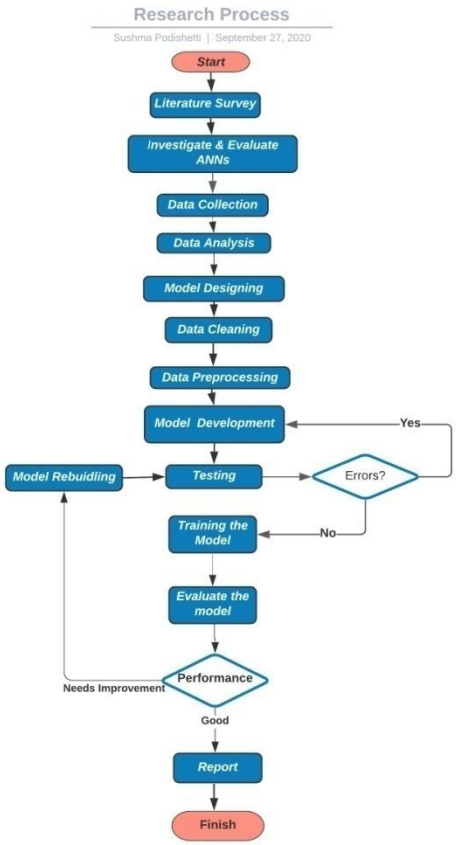

Figure 13 : Flow chart representing the research process

8. Requirements/Resources

The following resources would be required for the implementation of this research:

8.1 Hardware

A GPU is required to perform the training for the following reasons:

- As the dataset contains a large number of images.
- The number of epochs needed to train the model would be high to achieve better performance.
- Image segmentation includes complex operations to be performed internally.

8.2 Software

- Python 3.8. 5
- Pytorch

8.3 Technical skills

- Python
- Artificial Neural Networks
- Convolutional Neural Networks
- Conditional Generative Adversarial Networks
- U-Net

8.4 Domain Knowledge

- Brain tumors
- Types of brain tumors
- Gliomas
- Sub-regions of glioma
- MRI scan
- Types of MRI scans

9. Research Plan

The below figure shows the plan for this research represented in a Gantt chart.

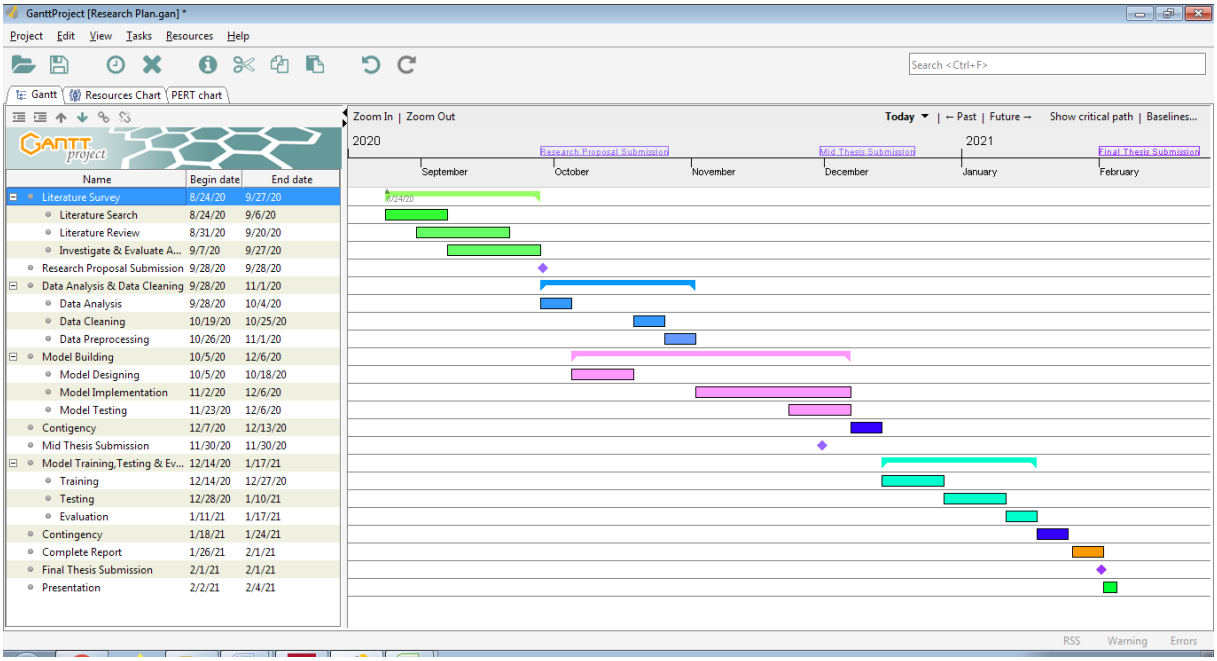

Figure 14 : Gantt chart showing the research plan.

Reference

Anon (2020) *Train Conditional Generative Adversarial Network (CGAN) - MATLAB & Simulink*. [online] Available at: https://www.mathworks.com/help/deeplearning/ug/train-conditional-generative-adversarial-network.html [Accessed 22 Sep. 2020].

Bakas, Spyridon; Akbari, Hamed; Sotiras, Aristeidis; Bilello, Michel; Rozycki, Martin; Kirby, Justin; Freymann, John; Farahani, Keyvan; Davatzikos, C., (2017) Segmentation Labels and Radiomic Features for the Pre-operative Scans of the TCGA-LGG collection. *Nat Sci Data*. [online] Available at: https://wiki.cancerimagingarchive.net/display/DOI/Segmentation+Labels+and+Radiomic+Features+for+the+Pre-operative+Scans+of+the+TCGA-LGG+collection#24282668197861a846e445a795694ff2a50eb66c.

Bakas, S., Akbari, H., Sotiras, A., Bilello, M., Rozycki, M., Kirby, J., Freymann, J., Farahani, K. and Davatzikos, C., (2017a) Segmentation labels and radiomic features for the pre-operative scans of the TCGA-GBM collection. The Cancer Imaging Archive. *Nat Sci Data*, 4, p.170117.

Bakas, S., Akbari, H., Sotiras, A., Bilello, M., Rozycki, M., Kirby, J.S., Freymann, J.B., Farahani, K. and Davatzikos, C., (2017b) Advancing The Cancer Genome Atlas glioma MRI collections with expert segmentation labels and radiomic features. *Scientific Data*, 4.

Bakas, S., Reyes, M., Jakab, A., Bauer, S., Rempfler, M., Crimi, A., Shinohara, R.T., Berger, C., Ha, S.M., Rozycki, M., Prastawa, M., Alberts, E., Lipkova, J., Freymann, J., Kirby, J., Bilello, M., Fathallah-Shaykh, H., Wiest, R., Kirschke, J., Wiestler, B., Colen, R., Kotrotsou, A., Lamontagne, P., Marcus, D., Milchenko, M., Nazeri, A., Weber, M.-A., Mahajan, A., Baid, U., Gerstner, E., Kwon, D., Acharya, G., Agarwal, M., Alam, M., Albiol, A., Albiol, A., Albiol, F.J., Alex, V., Allinson, N., Amorim, P.H.A., Amrutkar, A., Anand, G., Andermatt, S., Arbel, T., Arbelaez, P., Avery, A., Azmat, M., B., P., Bai, W., Banerjee, S., Barth, B., Batchelder, T., Batmanghelich, K., Battistella, E., Beers, A., Belyaev, M., Bendszus, M., Benson, E., Bernal, J., Bharath, H.N., Biros, G., Bisdas, S., Brown, J., Cabezas, M., Cao, S., Cardoso, J.M., Carver, E.N., Casamitjana, A., Castillo, L.S., Catà, M., Cattin, P., Cerigues, A., Chagas, V.S., Chandra, S., Chang, Y.-J., Chang, S., Chang, K., Chazalon, J., Chen, S., Chen, W., Chen, J.W., Chen, Z., Cheng, K., Choudhury, A.R., Chylla, R., Clérigues, A., Colleman, S., Colmeiro, R.G.R., Combalia, M., Costa, A., Cui, X., Dai, Z., Dai, L., Daza, L.A., Deutsch, E., Ding, C., Dong, C., Dong, S., Dudzik, W., Eaton-Rosen, Z., Egan, G., Escudero, G., Estienne, T., Everson, R., Fabrizio, J., Fan, Y., Fang, L., Feng, X., Ferrante, E., Fidon, L., Fischer, M., French, A.P., Fridman, N., Fu, H., Fuentes, D., Gao, Y., Gates, E., Gering, D., Gholami, A., Gierke, W., Glocker, B., Gong, M., González-Villá, S., Grosges, T., Guan, Y., Guo, S., Gupta, S., Han, W.-S., Han, I.S., Harmuth, K., He, H., Hernández-Sabaté, A., Herrmann, E., Himthani, N., Hsu, W., Hsu, C., Hu, X., Hu, X., Hu, Y., Hu, Y., Hua, R., Huang, T.-Y., Huang, W., Van Huffel, S., Huo, Q., HV, V., Iftekharuddin, K.M., Isensee, F., Islam, M., Jackson, A.S., Jambawalikar, S.R., Jesson, A., Jian, W., Jin, P., Jose, V.J.M., Jungo, A., Kainz, B., Kamnitsas, K., Kao, P.-Y., Karnawat, A., Kellermeier, T., Kermi, A., Keutzer, K., Khadir, M.T., Khened, M., Kickingereder, P., Kim, G., King, N., Knapp, H., Knecht, U., Kohli, L., Kong, D., Kong, X., Koppers, S., Kori, A., Krishnamurthi, G., Krivov, E., Kumar, P., Kushibar, K., Lachinov, D., Lambrou, T., Lee, J., Lee, C., Lee, Y., Lee, M., Lefkovits, S., Lefkovits, L., Levitt, J., Li, T., Li, H., Li, W., Li, H., Li, X., Li, Y., Li, H., Li, Z., Li, X., Li, Z., Li, X., Li, W., Lin, Z.-S., Lin, F., Lio, P., Liu, C., Liu, B., Liu, X., Liu, M., Liu, J., Liu, L., Llado, X., Lopez, M.M., Lorenzo, P.R., Lu, Z., Luo, L., Luo, Z., Ma, J., Ma,

K., Mackie, T., Madabushi, A., Mahmoudi, I., Maier-Hein, K.H., Maji, P., Mammen, C., Mang, A., Manjunath, B.S., Marcinkiewicz, M., McDonagh, S., McKenna, S., McKinley, R., Mehl, M., Mehta, S., Mehta, R., Meier, R., Meinel, C., Merhof, D., Meyer, C., Miller, R., Mitra, S., Moiyadi, A., Molina-Garcia, D., Monteiro, M.A.B., Mrukwa, G., Myronenko, A., Nalepa, J., Ngo, T., Nie, D., Ning, H., Niu, C., Nuechterlein, N.K., Oermann, E., Oliveira, A., Oliveira, D.D.C., Oliver, A., Osman, A.F.I., Ou, Y.-N., Ourselin, S., Paragios, N., Park, M.S., Paschke, B., Pauloski, J.G., Pawar, K., Pawlowski, N., Pei, L., Peng, S., Pereira, S.M., Perez-Beteta, J., Perez-Garcia, V.M., Pezold, S., Pham, B., Phophalia, A., Piella, G., Pillai, G.N., Piraud, M., Pisov, M., Popli, A., Pound, M.P., Pourreza, R., Prasanna, P., Prkovska, V., Pridmore, T.P., Puch, S., Puybareau, É., Qian, B., Qiao, X., Rajchl, M., Rane, S., Rebsamen, M., Ren, H., Ren, X., Revanuru, K., Rezaei, M., Rippel, O., Rivera, L.C., Robert, C., Rosen, B., Rueckert, D., Safwan, M., Salem, M., Salvi, J., Sanchez, I., Sánchez, I., Santos, H.M., Sartor, E., Schellingerhout, D., Scheufele, K., Scott, M.R., Scussel, A.A., Sedlar, S., Serrano-Rubio, J.P., Shah, N.J., Shah, N., Shaikh, M., Shankar, B.U., Shboul, Z., Shen, H., Shen, D., Shen, L., Shen, H., Shenoy, V., Shi, F., Shin, H.E., Shu, H., Sima, D., Sinclair, M., Smedby, O., Snyder, J.M., Soltaninejad, M., Song, G., Soni, M., Stawiaski, J., Subramanian, S., Sun, L., Sun, R., Sun, J., Sun, K., Sun, Y., Sun, G., Sun, S., Suter, Y.R., Szilagyi, L., Talbar, S., Tao, D., Tao, D., Teng, Z., Thakur, S., Thakur, M.H., Tharakan, S., Tiwari, P., Tochon, G., Tran, T., Tsai, Y.M., Tseng, K.-L., Tuan, T.A., Turlapov, V., Tustison, N., Vakalopoulou, M., Valverde, S., Vanguri, R., Vasiliev, E., Ventura, J., Vera, L., Vercauteren, T., Verrastro, C.A., Vidyaratne, L., Vilaplana, V., Vivekanandan, A., Wang, G., Wang, Q., Wang, C.J., Wang, W., Wang, D., Wang, R., Wang, Y., Wang, C., Wang, G., Wen, N., Wen, X., Weninger, L., Wick, W., Wu, S., Wu, Q., Wu, Y., Xia, Y., Xu, Y., Xu, X., Xu, P., Yang, T.-L., Yang, X., Yang, H.-Y., Yang, J., Yang, H., Yang, G., Yao, H., Ye, X., Yin, C., Young-Moxon, B., Yu, J., Yue, X., Zhang, S., Zhang, A., Zhang, K., Zhang, X., Zhang, L., Zhang, X., Zhang, Y., Zhang, L., Zhang, J., Zhang, X., Zhang, T., Zhao, S., Zhao, Y., Zhao, X., Zhao, L., Zheng, Y., Zhong, L., Zhou, C., Zhou, X., Zhou, F., Zhu, H., Zhu, J., Zhuge, Y., Zong, W., Kalpathy-Cramer, J., Farahani, K., Davatzikos, C., van Leemput, K. and Menze, B., (2018) Identifying the Best Machine Learning Algorithms for Brain Tumor Segmentation, Progression Assessment, and Overall Survival Prediction in the BRATS Challenge. [online] Available at: http://arxiv.org/abs/1811.02629.

Jiang, Z., Ding, C., Liu, M. and Tao, D., (2020) Two-stage cascaded u-net: 1st place solution to brats challenge 2019 segmentation task. In: *Lecture Notes in Computer Science (including subseries Lecture Notes in Artificial Intelligence and Lecture Notes in Bioinformatics)*. Springer, pp.231–241.

Lachinov, D., Shipunova, E. and Turlapov, V., (2020) Knowledge distillation for brain tumor segmentation. In: *Lecture Notes in Computer Science (including subseries Lecture Notes in Artificial Intelligence and Lecture Notes in Bioinformatics)*. pp.324–332.

Menze, B.H., Jakab, A., Bauer, S., Kalpathy-Cramer, J., Farahani, K., Kirby, J., Burren, Y., Porz, N., Slotboom, J., Wiest, R., Lanczi, L., Gerstner, E., Weber, M.A., Arbel, T., Avants, B.B., Ayache, N., Buendia, P., Collins, D.L., Cordier, N., Corso, J.J., Criminisi, A., Das, T., Delingette, H., Demiralp, Ç., Durst, C.R., Dojat, M., Doyle, S., Festa, J., Forbes, F., Geremia, E., Glocker, B., Golland, P., Guo, X., Hamamci, A., Iftekharuddin, K.M., Jena, R., John, N.M., Konukoglu, E., Lashkari, D., Mariz, J.A., Meier, R., Pereira, S., Precup, D., Price, S.J., Raviv, T.R., Reza, S.M.S., Ryan, M., Sarikaya, D., Schwartz, L., Shin, H.C., Shotton, J., Silva, C.A., Sousa, N., Subbanna, N.K., Szekely, G., Taylor, T.J., Thomas, O.M., Tustison, N.J., Unal, G., Vasseur, F., Wintermark, M., Ye, D.H., Zhao, L., Zhao, B., Zikic, D., Prastawa, M., Reyes, M. and Van Leemput, K., (2015) The Multimodal Brain Tumor Image

Segmentation Benchmark (BRATS). *IEEE Transactions on Medical Imaging*, 3410, pp.1993–2024.

Mirza, M. and Osindero, S., (2014) Conditional Generative Adversarial Nets. [online] Available at: http://arxiv.org/abs/1411.1784.

Myronenko, A., (2019) 3D MRI brain tumor segmentation using autoencoder regularization. In: *Lecture Notes in Computer Science (including subseries Lecture Notes in Artificial Intelligence and Lecture Notes in Bioinformatics)*. pp.311–320.

Ronneberger, O., Fischer, P. and Brox, T., (2015) U-net: Convolutional networks for biomedical image segmentation. In: *Lecture Notes in Computer Science (including subseries Lecture Notes in Artificial Intelligence and Lecture Notes in Bioinformatics)*. pp.234–241.

Singh, V.K., Romani, S., Rashwan, H.A., Akram, F., Pandey, N., Sarker, M.M.K., Abdulwahab, S., Torrents-Barrena, J., Saleh, A., Arquez, M., Arenas, M. and Puig, D., (2018) Conditional generative adversarial and convolutional networks for X-ray breast mass segmentation and shape classification. In: *Lecture Notes in Computer Science (including subseries Lecture Notes in Artificial Intelligence and Lecture Notes in Bioinformatics)*. pp.833–840.

APPENDIX C: SUMMARY OF BRATS 2012 TO 2019

The table below gives a summary of the top-ranking models in BraTS from 2012 to 2019.

No.	Year	Title	Method	Dataset	Results
1	2012	Segmentat-ion of Brain Tumour Images Based on Integrated Hierarchical Classification and Regularizatio-n	Integrated random forest classification with hierarchical conditional random field regularization in an energy minimization scheme	BraTS 2012	Edema / Tumour HGG (R): 0.61± 0.15 / 0.62± 0.27 LGG (R): 0.35± 0.18 / 0.49± 0.26 HGG(S): 0.68± 0.26 / 0.90± 0.06 LGG (S): 0.57± 0.24 / 0.74± 0.10 All: 0.59±0.24 / 0.73±0.22
2	2012	Context-sensitive Classification Forests for Segmentation of Brain Tumour Tissues	The segmentation was approached as a classification problem and was implemented using standard classification forests with spatially non-local features to represent the data	BraTS 2012	Edema / Tumour HGG (R): 0.70 ± 0.09 / 0.71± 0.24 LGG (R): 0.44 ± 0.18 / 0.62± 0.27 HGG(S): 0.65± 0.27 / 0.90± 0.05 LGG (S): 0.55± 0.23 / 0.71± 0.20
3	2013	ANTs and _Arboles	Advanced Normalization Tools (ANTs)[3] including its R packaging known as ANTsR. This includes a concatenation of RF models (one based on Gaussian mixture modelling (GMM), used as input to the succeeding one based on maximum a priority estimation and Markov random fields (MAP-MRF)).	BraTS 2013	Whole Tumour / Tumour Core / Enhancing Tumour Real: 0.88 / 0.76 / 0.55 Synthetic: 0.89 / 0.9 / 0

4	2013	Multi-class Abnormal Brain Tissue Segmentation Using Texture Features	Different brain tissues were characterized by using novel texture features such as piece-wise triangular prism surface area (PTPSA), and textons, along with intensity difference and regular intensity in multimodal MRI scans. Classical Random Forest (RF) classifier was used for segmentation and classification of the features in multi-modal MRI (T1, T2, Flair, T1 contrast) scans	BraTS 2013	<table><tr><th></th><th>Complete Tumour</th><th>Tumour Core</th><th>Enhancing Tumour</th></tr><tr><td>HGG</td><td>0.92±0.04</td><td>0.91±0.05</td><td>0.88±0.07</td></tr><tr><td>LGG</td><td>0.92±0.06</td><td>0.91±0.04</td><td>0.88±0.46</td></tr></table>
5	2014	Multi-modal brain tumour segmentation using deep convolutional neural networks	A voxel-wise classifier was employed. Predictions were based on local information provided by small 3D patches, one for each input channel. A Convolutional Neural Network was used for this task	BraTS 2013	<table><tr><th>Whole Tumour</th><th>Tumour Core</th><th>Enhancing Tumour</th></tr><tr><td>0.87</td><td>0.77</td><td>0.73</td></tr></table>
6	2014	Segmentation of Brain Tumour Tissues with Convolutional Neural Networks	A standard CNN implementation based on multi-channel 2D convolutions and adapted in such a way that it operates on multichannel 3D data usually	BraTS 2013	<table><tr><th>Whole Tumour</th><th>Tumour Core</th><th>Enhancing Tumour</th></tr><tr><td>0.837±0.094</td><td>0.736±0.256</td><td>0.690±0.249</td></tr></table>

7	2015	A convolutional neural network approach to brain lesion segmentation	2D CNN-based model with a cascaded architecture, for modelling the local dependency of labels. Two parallel CNNs were used to extract either the local details or global context of tissue appearance of the input patches	BraTS 2013	Whole Tumour 0.88 Tumour Core 0.79 Enhancing Tumour 0.73
8	2015	Structured Prediction with Convolutional Neural Networks for Multimodal Brain Tumour Segmentation	A patch-based local structure prediction approach using 2D CNN. For each subtask, 2D image feature patches were extracted and fed to a CNN to predict the most likely label patches located in the centre of each image patch.	BraTS 2014	Whole Tumour 0.83±0.13 Tumour Core 0.75±0.2 Enhancing Tumour 0.77±0.18
9	2016	DeepMedic on Brain Tumour Segmentation	DeepMedic model consisting of an 11-layer 3D CNN with residual connections. It had two parallel pathways, each of which processed the input at a specific scale.	BraTS 2015	Whole Tumour 0.896 Tumour Core 0.754 Enhancing Tumour 0.718
10	2016	Improving boundary classification for brain tumour segmentation and	CNN architecture, but the differentiating feature was the definition of the loss function and investigation of the impact of the choice of loss function on segmentation	BraTS 2016	Whole Tumour 0.89 Tumour Core 0.76 Enhancing Tumour 0.72

		longitudinal disease progression	accuracy. To enhance the accuracy of segmentation around edges, they introduced a modified version of the cross-entropy loss function, which weighted pixels based on their proximity to pixels of other classes.		
11	2017	Ensembles of multiple models and architectures for robust brain tumour segmentation	Ensembles of multiple models and architectures (EMMA) is an ensemble of DeepMedics, fully convolutional network models (FCN, U-nets.	BraTS 2017	Whole Tumour / Tumour Core / Enhancing Tumour Validation set: 0.901 / 0.797 / 0.738 Test set: 0.886 / 0.785 / 0.729
12	2017	Automatic Brain Tumour Segmentation using Cascaded Anisotropic Convolutional Neural Networks	A triple cascaded framework of fully convolutional neural networks (whole tumour (WNet), tumour core (TNet) and enhancing tumour core (ENet))was proposed to segment the sub-regions sequentially according to the hierarchy. The network comprised of multiple layers of anisotropic and dilated convolution filters and was combined with multi-view fusion to minimize the false positives.	BraTS 2017	Complete Tumour / Tumour Core / Enhancing Tumour Without multi-view Fusion (Validation set): 0.8896 / 0.8255 / 0.7411 With multi-view Fusion (Validation set): 0.905 / 0.8378 / 0.7859 Test set: 0.8739 / 0.7748 / 0.7831

13	2018	3D MRI brain tumour segmentation using autoencoder regularization	A semantic segmentation network for tumour subregion segmentation from 3D MRIs based on encoder-decoder architecture.	BraTS 2018	Validation dataset	Complete Tumour 0.9100	Tumour Core 0.8668	Enhancing Tumour 0.8233
					Test dataset	0.8839	0.8154	0.7664
14	2018	No New-Net	A 3D U-net with minor modifications well trained with large patch size. The model used region-based training, co-training with additional training data, postprocessing to target false positive enhancing tumour detection as well as a combination of Dice and cross-entropy loss which substantially increased its performance.	BraTS 2018	Validation dataset	Complete Tumour 91.26	Tumour Core 86.34	Enhancing Tumour 80.87
					Test dataset	87.81	80.62	77.88
15	2019	Two-Stage Cascaded U-Net: 1st Place Solution to BraTS Challenge 2019 Segmentation Task	A novel two-stage cascaded U-Net to segment the substructures of brain tumours from coarse to fine.	BraTS 2019	Validation dataset	Complete Tumour 0.90941	Tumour Core 0.86473	Enhancing Tumour 0.80211
					Test dataset	0.88796	0.83697	0.83267

16	2019	Bag of Tricks for 3D MRI Brain Tumour Segmentation	Different kinds of tricks applied to 3D brain tumour segmentation with DNN. Tricks were divided into three main categories: data processing methods including data sampling, random patch-size training, and semi-supervised learning, model devising methods including architecture devising and result fusing, and optimizing processes including warming-up learning and multi-task learning	BraTS 2019		Complete Tumour	Tumour Core	Enhancing Tumour
					Validation dataset	0.910	0.835	0.754
					Test dataset	0.883	0.861	0.81